RUSSIAN JOURNAL OF EARTH SCIENCES, VOL. 3, NO. 3, PAGES 197–217, AUGUST 2001

Evolution of magmatism in the zone of junction between granite–greenstone and granulite–gneiss regions, Sayan mountains, Siberia

V. I. Levitskii and G. P. Sandimirova

Vinogradov Institute of Geochemistry, Siberian Division, Russian Academy of Sciences

A. I. Melnikov

Institute of the Earth's Crust, Siberian Division, Russian Academy of Sciences

Abstract. The crust in the south of the Siberian Craton includes the tonalite-trondhjemite complex of the basement, the highly metamorphozed rocks of the Kitoi Suite, the rocks of the Onot greenstone belt, ultrametamorphic rocks, the gabbroids of the Arban Complex, the metaultramafics of the Ilchira Complex, the rocks of the postultrametamorphic phase, and the metasomatic rocks of deep fault zones. The continental sialic tonalite-trondhjemite crust and the oceanic basaltic crust coexisted during the Early Archean. The rocks of the Onot greenstone belt are restricted to the linear troughs (paleorifts) of the early sialic tonalite-trondhjemite crust. The bottom of the belt is dominated by calc-alkalic bimodal rocks, the middle, by carbonate rocks, and the top, by clastic rocks and flysch. The processes of ultrametamorphic and postultrametamorphic allochemical transformations altered significantly the preexisting rocks. The junction zones of the Baikal granulite-gneiss and East Sayan granite-greenstone regions are marked by the wide development of the rapakivi-like granites of the Shumikha Complex, similar petrogeochemically to the maritime complex of the West Baikal region. The subconcordant linear distribution of the rocks of the Onot Belt, the ultrametamorphic and postultrametamorphic rocks, the granites of the Shumikha Complex, and the metasomatic rocks of deep fault zones testifies to their long-lasting connections with mantle sources.

Introduction

Granite–greenstone and granulite–gneiss regions are classified among the main geostructural elements of the Precambrian continental crust, and the establishment of relations between these low- and high-grade metamorphic formations is a fundamental problem of modern geology. The main aim of this paper is to discuss regular mechanisms in the operation and evolution of petrogenic processes in the zone of junction between the East Sayan granite–greenstone region (using the largest Onot greenstone belt as an example) and the high-grade metamorphic rocks of the Sharyzhalgai Complex of the Baikal granulite–gneiss province in the southern marginal salient of the Siberian Craton basement (the interfluvial area of the Kitoi, Bolshaya and Malaya Belaya, Onot, and Tagna rivers in the Southeast Sayan region).

Earlier a wide development of tonalite–trondjemite rock associations was discovered there [*Sandimirova et al.,* 1992]. Geochronological and isotopic studies were carried out [*Levitskii et al.,* 1995; *Sandimirova et al.,* 1992, 1993]. The compositions of the basement rocks and some of the Onot Greenstone Belt rocks were determined [*Mekhonoshin,* 1999; *Nozhkin et al.,* 1995; and others]. The origin and petrochemistry of ores in the Onot mineral deposit were estab-

Paper number TJE01063.
ISSN: 1681–1208 (online)

The online version of this paper was published August 21, 2001.
URL: http://rjes.agu.org/v03/TJE01063/TJE01063.htm

lished [*Levitskii,* 1994], and the granites of the Shumikha Complex were classified as rapakivi-like granites [*Levitskii et al.,* 1997a, 1997b]. The aim of this paper is to generalize and summarize the earlier and new evidence on the geology, geochronology, petrology, and geochemistry of the region.

Methods of Study

The main aim of the investigations discussed was to study the rocks of different origins, reveal relationships between, and investigate their geological, petrological, mineralogical, and geochemical evolution. As a result of this work, the following associations of rocks were distinguished: (1) igneous rocks; (2) metamorphic rocks which had experienced isochemical transformations; (3) ultrametamorphic rocks, represented by plagioclase and K-feldspar migmatites and granitoids in the aluminosilicate substrate and by skarn in the marble: (4) metasomatic rocks of the postultrametamorphic stage (post-migmatitic metasomatic rocks after *Glebovitskii and Bushmin,* [1983]) and of the deep fault zones. The postultrametamorphic rocks developed under the conditions of declining temperature and are usually subdivided into subclasses of different temperatures, which are not discussed here.

The geochronological investigations and analytical work done in the Vinogradov Institute of Geochemistry can be summarized as follows: Rb-Sr isochron analysis (analysts G. P. Sandimirova and Yu. A. Pakholchenko); X-ray fluorescence analysis of petrogenic elements and Ba, Sr, and Zr (analysts T. N. Gunicheva and A. L. Finkelshtein); atomic absorption analysis (Li, Rb, Cs, analyst D. Ya. Orlova); quantitative spectral analysis (La, Ce, Nb, Yb, Y, Co, Ni, Cr, V, Sc, Zr, Sn, Mo, Zn, Pb, B, Ge, Ag, Ba, Sr, F, B, and Be, analysts E. B. Smirnova, L. N. Odareeva, A. I. Kuznetsova, S. K. Yaroshenko, and L. L. Petrov); scintillation analysis (Au, Pd, analyst S. I. Prokopchuk). In this work we also used the REE analyses performed using the methods of preliminary sample enrichment and quantitative spectral analysis in the Vinogradov Institute of Geochemistry (analysts L. I. Chuvashova and E. V. Smirnova) and the method of instrumental neutron activation analysis in the Institute of Geology and Geophysics, Siberian Division, Russian Academy of Sciences (analyst V. A. Bobrov) [*Nozhkin et al.,* 1995].

Geochronological methods. The samples were prepared chemically for the isotopic analyses using one specimen, the decomposition by a ($HF+HNO_3+HClO_4$) mixture, and two stages of Rb and Sr partitioning by the method of ion-exchange chromatography using a BiORad AG 50 W×8 (200–400-mesh) cation exchanger in an H+ form. Isotope compositions were measured on a MI 1201T mass spectrometer completed with a PRM-2 unit and an Iskra-1256 microcomputer using a mode of one-ribbon source. To enhance the ionization effect and stabilize the ion beam, the specimen was applied to the ribbon using a $Ta_2O_5 \times n\ H_2O$-based activator in the form of a suspension in ($HF+HNO_3+H_3PO_4$) acids in a ratio of 1:1:1 [*Tauson et al.,* 1983]. The concentrations of rubidium were determined by the method of isotope dilution, and those of strontium, by the method of double isotope dilution. The validity of the isotopic analyses was estimated using SRM-987, VNIIM-Sr, and ISG-1 (granite) standards. The isochron parameters, such as the Rb/Sr ages and primary $(^{87}Sr/^{86}Sr)_0$ ratios were calculated using the Isoplot computer program [*York,* 1966] and a polynomial method using models [*McIntyre et al.,* 1966] taking into account $\pm 2\sigma$ errors for both axes of the coordinates (0.5% for $^{87}Rb/^{86}Sr$ and 0.05% for $^{87}Sr/^{86}Sr$).

Analytical methods. The lower limits of detecting petrogenic elements (Si, Ti, Al, Fe, Mn, Mg, Ca, P, Na, and K) were 0.01%. Those for trace elements (ppm) were 5–10 for Zr, Ba, Sr, and Zn; 0.5–1 for Li, Rb, Cs, and Pb; 0.1–15 for La, Ce, Nb, Yb, and Y (direct quantitative spectral analysis), and 0.01–1 (instrumental neutron activation analysis); 1 for Co, Ni, V, and Sc; 3 for Cr; 5 for Cu; 0.8 for Sn and Ge; 1–5 for B; 100 for F; 0.05 for Be; 0.3 for Mo; 0.01–1 for Ta, Nb, and Hf (spectrochemical analysis with preliminary enrichment); 0.01 for Ag; and 0.0001 for Au and Pd. The analytical procedures were described in the literature [*Emission...,* 1976; *Finkelshtein and Afonin,* 1996; *Smirnova and Konusova,* 1982; and others]. We verified our analytical results using international and Russian standards: BCR, ST-1A, SGD-1A, AGV-1, G-2, SM, SG-1A, SG-2, SI-1, BM, TB, KH, GXR 1-5, and others, and also using repeated analyses of the same elements in selected samples by different methods, in different laboratories, and in different institutes. The correlation of the results of analyzing petrogenic, trace, and rare-earth elements was done repeatedly and showed good agreement [*Levitskii,* 2000; *Petrova,* 1990]. The representativeness of the samples and the reliability of the analytical data were high enough to derive the trustworthy geochemical characteristics of the rocks.

Data

The main geostructural elements of the crust in the Sharyzhalgai salient of the Siberian Craton basement are the Baikal granulite–gneiss region and the East Sayan granite–greenstone region. Generally, the junction between these high-and low-grade metamorphic rock regions is marked by faults and, in some areas, by imbricate structures, as reported by previous investigators [*Shafeev, et al.,* 1981]. Usually, the stratigraphic units and complexes have tectonic contacts with the rocks of higher TP values resting on the lower-grade metamorphic rock strata.

The Baikal granulite–gneiss region was not classified earlier as an individual geostructural element of the Precambrian crust. In our understanding, this region includes the outcrops of the granulite facies rocks in the Irkut, Zhidoi, Kitoi, Bulun [*Grabkin and Melnikov,* 1980; *Levitskii et al.,* 2000], and other blocks of the Sayan marginal salient of the Siberian Craton basement (Figure 1).

The rocks of the Sharyzhalgai Series dominate in the Irkut and Zhidoi blocks in the belt stretching from the Katoi River to the Baikal Lake shore between Kultuk town and Port

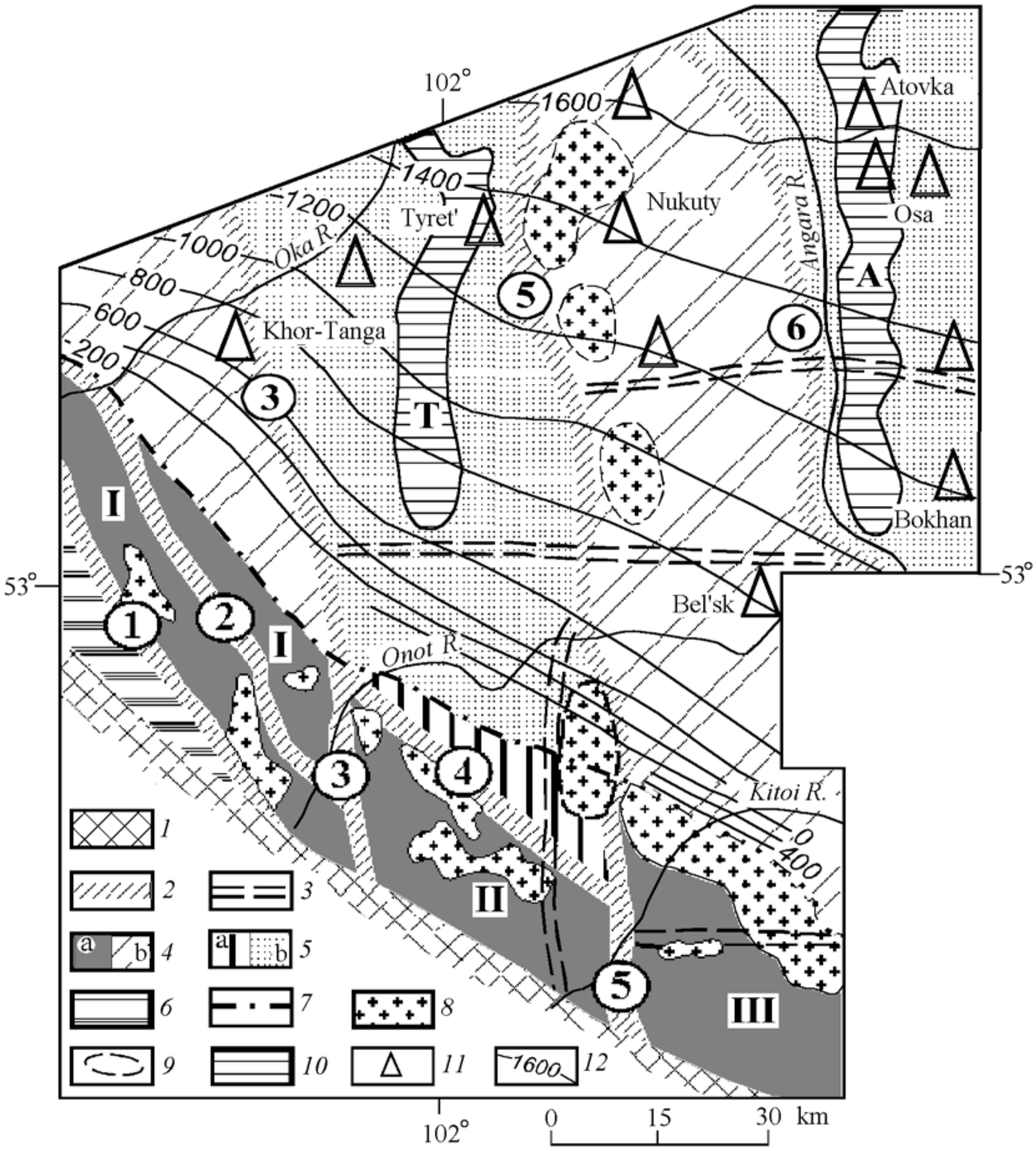

Figure 1. Schematic map on the basement of the study area prepared from geological and geophysical data [*Lobachevskii and Melnikov,* 1985].
(1) Main Sayan Fault zone; (2) large interblock faults (figures in circles): (1) Tocher, (2) Alar, (3) Onot–Khortagna, (4) Savina, (5) Kitoi–Zalari, and (6) Angara; (4) The rocks of the Baikal granulite-gneiss region: (a – exposed on the Sharyzharlgai salient and on the Bulun (I), Kitoi (II), and Zhidoi (III) blocks; b – covered by sediments); (5) Late Archean rocks of the Onot Belt: (a) exposed, (b) covered by sediments; (6) Proterozoic rocks of the Urik–Iya trough; (7) Present-day boundary of the craton's sedimentary cover; (8) granitoids of the Shumikha (Sayan) Complex; (9) granitoid bodies mapped from gravity data under the craton's sediments; (10) inferred basement rises: (A) Atovka, (T) Tyret; (11) deep drill holes; (12) isobases (m) of the top of the Mot Formation.

Baikal. This area was described by many geologists [*Evolution...,* 1988; *Grabkin and Melnikov,* 1980; *Petrova,* 1990; *Petrova and Levitskii,* 1984; and others]. The age of the early metamorphism, derived in the laboratories of the Institute of Geochemistry and the Institute of the Earth's Crust in different periods of time by the Rb-Sr isochron method for basic two-pyroxene schists ranges between 3.72±0.3 and 3.1 Ga [*Gornova and Petrova,* 1999; *Mekhonoshin et al.,* 1987; *Sandimirova et al.,* 1979; and others]. The high-precision zircon dating and the Rb/Sr and Nd/Sm data [*Aftalion et al.,* 1991; *Bibikova et al.,* 1990] yielded a broad range of values: from 2.84±0.72 to 1.8±0.30 Ga. However,

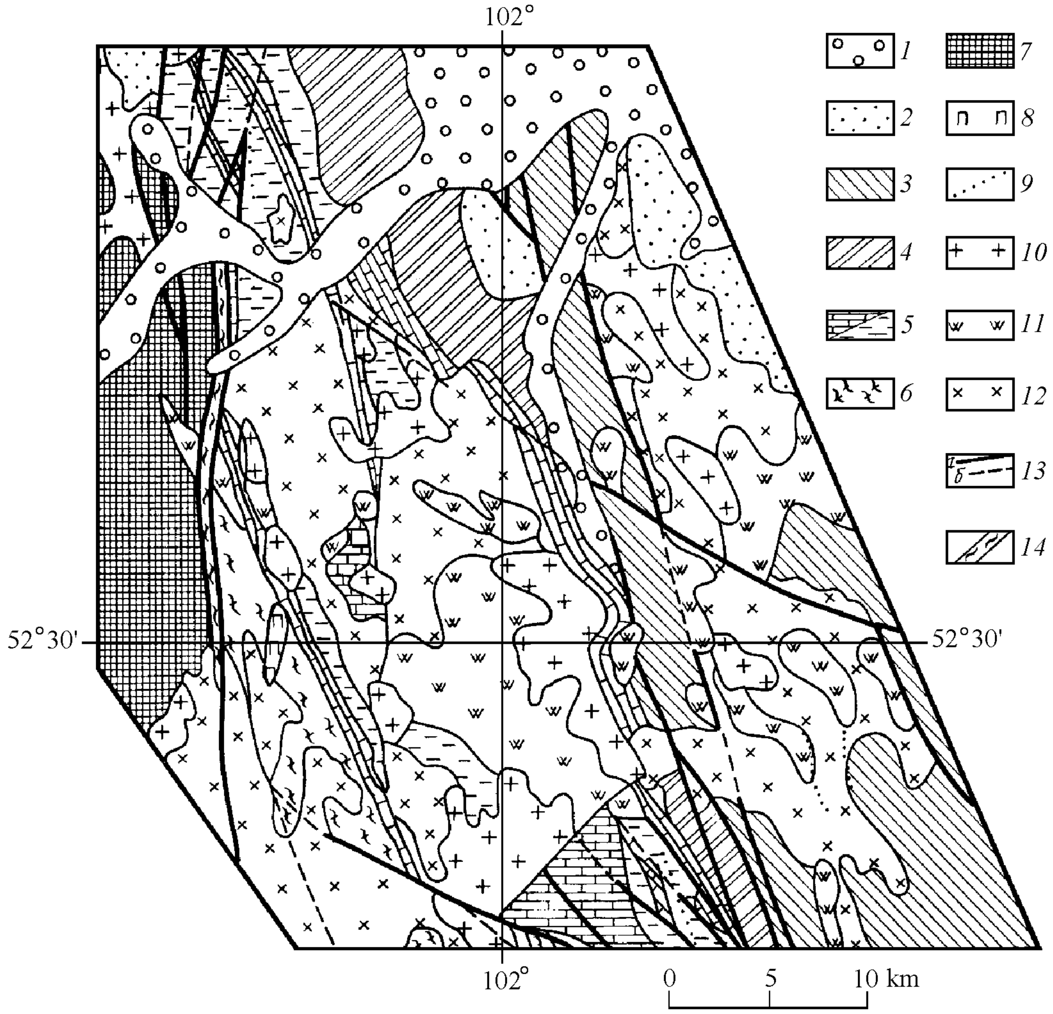

Figure 2. Schematic geological map of the Onot greenstone belt reproduced from [*Nonmetallic...*, 1984]. (1) alluvium; (2) red beds of the Ushakovskaya Formation; (3–6) Onot greenstone belt: Sosnovyi Baits Suite (3), the upper subsuite of the Kamchadal Suite (4), the lower subsuite of the Kamchadal Suite (5): mainly carbonate (a) and mainly noncarbonate (b) rocks, Maloiret and Burukhtui suites (6); (7) Kitoi Series; (8) peridotites and pyroxenites of the Il'chir Complex; (9) dolerites of the Nerchinsk Complex; (10) granitoids of the Shumikha Complex; (11) gabbro, gabbro-diabase, and apogabbro amphibole rocks of the Arban Complex; (12) tonalites and trondjemites of the basement of the Onot Belt and ultrametamorphic rocks (migmatites and granites) developed after them; (13) faults: (a – proved, b – inferred); (14) deep fault zones.

all of these dates were obtained for the rocks of the ultrametamorphic stage. Moreover, M. Aftalion et al. [1991] analyzed altered rocks and do not mention any analyses for the primary rocks.

The metamorphic rocks of the Kitoi Series, developed in the Bulun and Kitoi blocks (Figure 1 and 2), are medium-Al, with biotite, amphibole, pyroxene, and garnet, and high-Al, with sillimanite, cordierite, biotite, and garnet, plagiogneisses and two-pyroxene plagioschists and plagiogneisses (occasionally with garnet), metagabbro-anorthosites, dolomite and calcite marbles, and less common sillimanite and biotite quartzitic gneisses and monomineral quartzite. The compositions of these rocks are given in Table 1 and their REE distribution patterns, in Figure 3c. The age of the Kitoi plagiogneisses was found to be 2.827±180 Ga with $(^{87}Sr/^{86}Sr)_0 = 0.7055 \pm 20$.

The rocks of the ultrametamorphic stage cut the metamorphic rocks, contain their relicts, and show often observed transitions from the unaltered early rocks via plagiomigmatite, K-feldspar, and schlieric K-feldspar migmatites to autochthonous and allochthonous granites. The compositions of these rocks are presented in Table 2. Compared to their parental rocks, they are lower in iron, CaO, MgO, Li, F, iron-group elements, and Tb and higher in SiO_2, K_2O, Rb, Ba, light REE, Zr, and Pb (Table 2, Figure 3c). A se-

Table 1. Chemical compositions (wt.%) and the contents of minor and rare-earth elements (ppm) in the metamorphic rocks of the Kitoi Series

no.	1(1)	2(1)	3(1)	4(1)	5(3)	6(2)	7(2)	8(1)	9(6)	10(1)	11(1)
SiO_2	48.35	78.21	89.84	0.92	55.74	66.7	57.72	68.71	64.4	54.96	51.07
TiO_2	1.18	0.21	0.1	0.4	1.77	0.69	2.41	0.6	0.77	0.29	1.24
Al_2O_3	19.08	8.91	3.78	0.26	13.22	15.05	14.67	12.93	14.65	5.47	13.01
FeO	12.88	2.18	1.01		12.31	5.70	10.10	6.67	8.74	10.64	15.12
MnO	0.16			0.77	0.14	0.07	0.11	0.08	0.05	0.19	0.21
MgO	6.16	5.06	2.75	0.9	3.96	2.08	2.98	2.83	3.33	10.41	6.09
CaO	1.88	0.26	0.09	53.83	7.73	3.01	5.07	1.43	1.72	5.14	8.64
P_2O_5		0.02	0.02	0.05	0.39	0.16	0.42	0.07	0.09	0.03	0.11
K_2O	1.24	2.81	1.46	0.04	2.19	2.14	2.86	2.52	2.07	0.57	0.84
Na_2O	5.32	1.16	0.37	0.12	1.98	3.15	2.76	2.47	2.24	0.84	2.16
LOI	4.06	1.09	0.57	41.78	0.53	1.085	0.405	1.5	1.835	1.55	1.56
Li	18	4	3	0.1	22	36	36	22	49	64	14
Rb	22	140	65	0.1	47	89	92	13	114	16	42
Cs	1	4	0.1		2	2	2	2	4		0,1
Ba	10	330	170	14	410	597	710	330	395	69	80
Sr	145	70	20	100	243	412	440	195	110	47	120
B				1	7	20		10	11	22	2
Be				0.15	1.35	2		3	2.35	0.45	0.8
F				230	875				1000	370	
Mo				1	0.5	3		1.5	1.9	0.5	0.2
Sn				2.9	4	1.5		0.5	2.1	1.7	0.5
La				5	25	30		22	38	2	3
Ce				20	69	60		52	74	3	30
Nd				5	48			29	34	2	21
Yb				0.1	4.15	3		2.2	2.5	1.5	3.8
Y				9	37	30		17	3	11	25
Zr	235	430	210	25	186	275	281	170	255	60	50
Zn					246	180		100	73	145	150
Pb				0.5	8	20		2	18	1	3
Cu	7			2	62	60		80	56	14	80
Cr	240			5	39	150		150	210	1300	80
V	240			7	290	80		80	170	120	400
Ni	150			9	73	100		100	120	390	80
Co	45			0.5	37	20		20	36	65	5
Sc	43			2	50	20		2	37	16	30

Note: Here and in the tables that follow the number of analyses used to calculate the mean values is given in the parentheses. 1) metagabbro anorthosite; 2) sillimanite–biotite quartzitic gneiss; 3) biotite–muscovite quartzite; 4) calcite marble; 5) apoandesite plagiogneiss with biotite, amphibole, and pyroxene; 6) biotite plagiogneiss; 7) melanocratic biotite plagiogneiss; 8) garnet–biotite plagiogneiss; 9) plagiogneiss with sillimanite, cordierite, and biotite; 10) sillimanite gneiss; 11) two-pyroxene plagioschist with amphibole.

ries of isochrons with ages ranging between 2.6 and 2.2 Ga was derived for the different types of the migmatites and autochthonous and allochthonous granitoids of the Kitoi Series [*Sandimirova et al.,* 1993].

The rocks of the postultrametamorphic phase are represented mainly by amphibole- and to a lesser extent by scapolite-, biotite-, epidote-, and zoisite-bearing rock assemblages. They make up bodies of an irregular and a vein form, are often restricted to contacts between contrasting rocks, and commonly trace fault zones.

The East Sayan granite-greenstone region borders the Baikal granulite-gneiss region along fault zones. The discovery of plagiogranites with an age of 3.25 Ga along the Onot River [*Bibikova et al.,* 1982] was the first evidence which justified the idea of the wide development of tonalite–trondjemite associations and greenstone belts in this region. Later, the East Sayan Superbelt was distinguished on the basis of geological and structural data [*Evolution...,* 1988]. Recently the term "East Sayan granite–greenstone region" became very popular [*Nozhkin et al.,* 1995]. Based on the sum total of the geostructural, geochronological, petrological, and geochemical data, this region includes: (1) the rocks of an infrastructure–the oldest tonalite–trondjemite associations of the basement complex and (2) the rocks of a suprastructure, which compose the Onot, Targozoi, Monkres, and other extensive greenstone belts which differ in the collection and ratio of their rock associations (Figure 1 and 2).

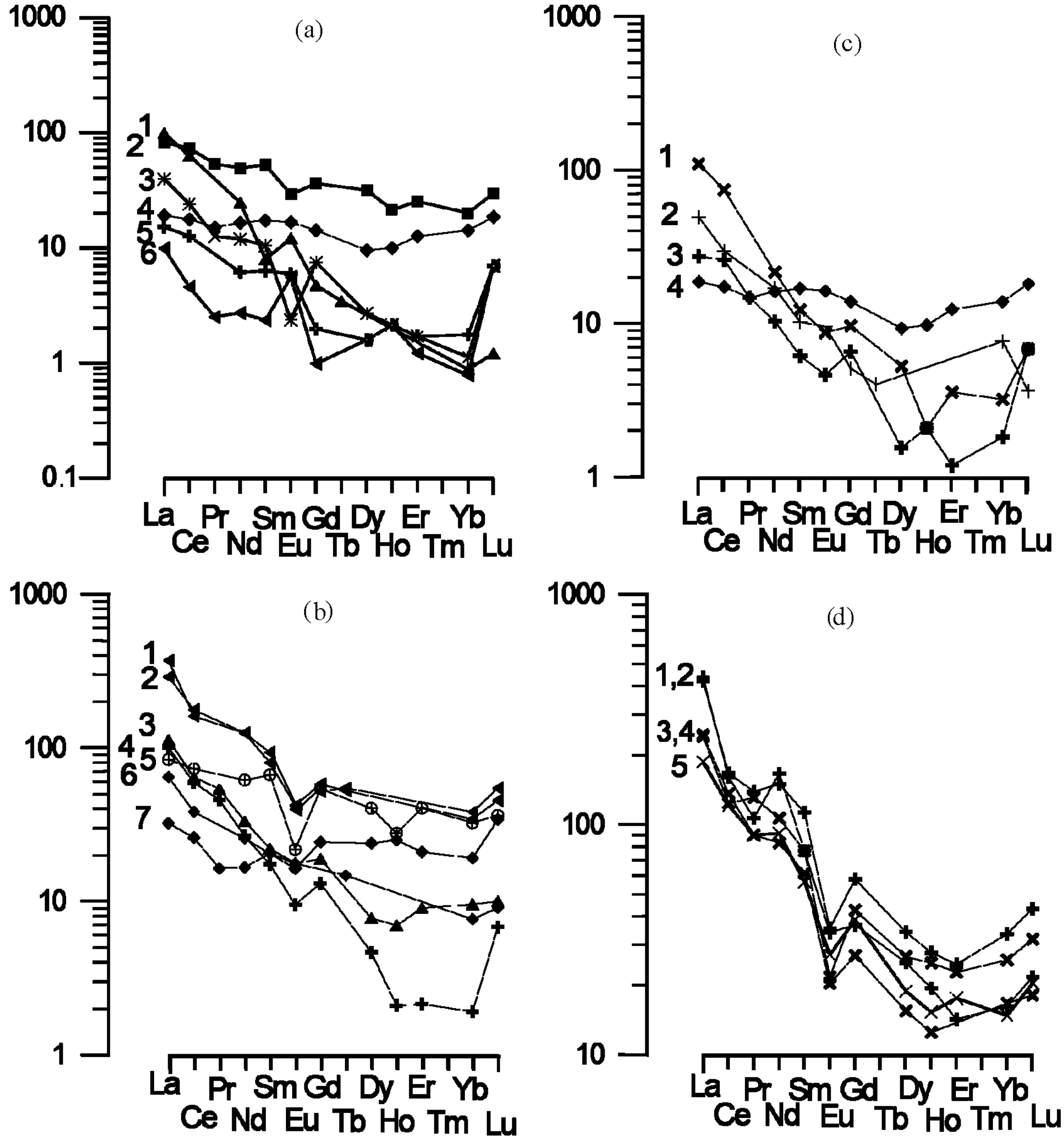

Figure 3. Distributions of rare earth elements, chondrite-normalized.
Basement complex (a): (1) apotonalite amphibole–biotite plagiogneiss, (2) plagioclasite, (3) K-feldspar granite-pegmatite, (4) amphibolite, (5) K-feldspar leucocratic granite, (6) trondjemite. Onot greenstone belt (b): (1–2) biotite-amphibole plagiogneiss, (3) apodacite biotite plagiogneiss, (4) biotite granite, (5) biotite–garnet–amphibole rock of the postultrametamorphic stage, (6) amphibolite of Kamchadal Suite, (7) amphibolite of Maloiret Suite. Kitoi Series (c): (1) shlieric K-feldspar migmatite, (2) biotite granite, (3) leucocratic granite, (4) amphibolite. Shumikha Complex (d): (1, 2) amphibole–biotite granodiorite of phase 1, (3) granosyenite and (4) granite porphyry of phase 3, (5) granite-pegmatite.

The gray-gneiss complex of the basement is represented by metatonalite biotite–amphibole plagiogneisses with minor lenticular amphibolite inclusions. There are early banded trondjemites (type 1), which occur as massifs ranging between 1–5 and 20–28 km in length and are traceable from the Onot R. to the Savina R., and late cross-cutting bodies of massive trondjemite and tonalite (type 2). The compositions of these rocks are presented in Table 3. The age of their emplacement, derived earlier from the trondjemites of types 1 and 2, was found to be 3.711±0.26 Ga with $(^{87}Sr/^{86}Sr)_0 = 0.698 \pm 0.001$ [*Sandimirova et al.,* 1992]. Based on the data available for the metatonalite plagiogneiss and trondjemite of type 1, the age of the rocks was found to be 3.113±0.0039 Ga with $(^{87}Sr/^{86}Sr)_0 = 0.7004 \pm 0.0005$ (our data, in press). The petrography, petrology, and geochemistry of the tonalite–trondjemite associations were described earlier [*Nozhkin et al.,* 1995; *Sandimirova et al.,* 1992]. Plagiogneisses and trondjemites from the basement of

Table 2. Chemical compositions (wt.%) and the contents of minor and rare-earth elements (ppm) in the ultrametamorphic rocks of the Kitoi Series

no.	1(1)	2(1)	3(1)	4(2)	5(4)	6(7)	7(4)	8(3)	9(4)	10(4)	11(7)	12(1)
SiO_2	75.15	77.14	71.75	55.19	66.79	74.03	73.14	74.29	75.28	75.39	75.27	73.00
TiO_2	0.03	0.20	0.36	1.05	0.61	0.29	0.19	0.08	0.26	0.13	0.06	0.02
Al_2O_3	11.50	11.96	14.26	12.21	14.80	13.08	14.14	13.98	11.79	12.48	13.16	14.63
FeO	4.30	2.44	3.04	10.57	5.99	2.64	1.74	0.44	3.50	2.41	1.28	0.60
MnO	0.09	0.02	0.04	0.18	0.07	0.04	0.03	0.17	0.03	0.03	0.02	0.01
MgO	0.80	0.07	0.89	5.82	2.32	0.42	0.37	0.13	0.22	0.21	0.14	0.07
CaO	1.50	0.98	1.54	8.00	3.79	1.33	1.12	0.63	0.74	0.52	0.49	0.34
P_2O_5	0.02	0.02	0.06	0.11	0.12	0.07	0.06	0.04	0.04	0.04	0.04	0.02
K_2O	2.40	2.23	3.58	1.33	1.56	3.97	5.43	7.18	4.86	5.41	6.10	8.76
Na_2O	2.77	4.68	3.39	4.35	3.54	3.39	3.23	2.70	2.78	2.84	3.04	2.27
LOI	0.89	0.16	0.84	1.305	0.97	0.54	0.42	0.41	0.4	0.475	0.35	0.14
Li	54	1	10	10	14	14	10	5	11	6	4	3
Rb	104	65	12	45	70	130	150	175	183	189	194	240
Cs		0.10	0.50	2.00	2.00	0.40	1.05		1.30	1.75	1.02	2.00
Ba	590	460	1395	230	325	827	605	1400	745	515	569	740
Sr	100	20	325	215	245	184	240	100	35	53	101	250
B	7		15	14	12	8	12	13			13	
Be	2.20		2.00	5.35	1.60	2.55	1.65	1.18			0.79	
F	400			1300	280	483	240	390			169	
Mo	0.50		1.50		0.50	3.67	0.35	0.75			0.83	
Sn	4.40		2.00	4.80	2.40	5.03	3.45	1.05			1.35	
La	120		120	25	62	79	64	13	190		7	
Ce	140		220	55	120	141	117	31	320		18	
Nd	80		80	26	25	54	59	9	120		6	
Yb	13.00		1.60	4.85	1.70	4.85	2.65	1.35	6.20		1.69	
Y	77		18	35	21	43	29	14	47		12	
Zr	440	330	325	185	145	266	118	63	355	223	91	10
Zn	107		60	100	50	160	54	2			8	
Pb	27		2	10	28	36	32	47			55	
Cu	11		1	100	18	9	4	2	14		11	
Cr	32		15	74	49	19	11	11	20		6	
V	23		30	310	95	9	7	4	26		3	
Ni	30		10	38	18	12	4	8	12		5	
Co	6		5	54	18	3	4	1	10		3	
Sc	17		4			7	5	2	8		2	

Note: 1) biotite–cordierite plagiomigmatite; 2) biotite–amphibole plagiomigmatite; 3) schlieric garnet–biotite migmatite; 4) amphibole and pyroxene plagiomigmatites; 5) schlieric plagiomigmatite with biotite and amphibole; 6) K-feldspar migmatite with biotite, amphibole, and cordierite; 7) schlieric K-feldspar biotite migmatite; 8) paraautochthonous granite with biotite and amphibole; 9) autochthonous granite with biotite and amphibole; 10) paraautochthonous granite with biotite and garnet; 11) leucocratic allochthonous granite; 12) pegmatite. The primary rocks for (1–2), (6–7), and (9–10) were pelitic gneisses; plagiogneiss for (3), schist for (4–5, 8), migmatite for (11), and granite for (12).

the Onot greenstone belt, and from the other regions of the world [*Trondjemites, Dacites...*, 1983] show abnormally low mantle ratios $(^{87}Sr/^{86}Sr)_0$ and positive Eu anomalies (Figure 3a). As follows from the regional maps of magmatism and correlation, the tonalite–trondjemite associations with and without K-feldspar correlate with the plagiogranites and plagiogneisses of the Onot Complex (Figure 2).

The rocks of the ultrametamorphic phase occur as crosscutting veins, nests, or zones of biotite and amphibole–biotite plagioclase–K-feldspar and K-feldspar migmatites, and autochthonous, paraauthochthonous, and allochthonous, usually leucocratic granites. Less common are veins of coarse-grained and pegmatoid rocks consisting largely or even solely of plagioclase, known as plagioclasite, and also K-feldspar or plagioclase pegmatites. The bodies of relict tonalite blocks in the migmatites and granites range between (1×3) and (100×1000) m in size. They differ from the original rocks of the tonalite–trondjemite association by their higher contents of SiO_2, Al_2O_3, K_2O, Rb, Ba, Cs, Zr, Pb, and light REE (Figure 3a) and by their lower contents of F, MgO, CaO, Li, Yb, Y, Cu, V, Ni, Co, Sc, and in some cases of Na_2O (Table 3).

Table 3. Chemical compositions (wt.%) and the contents of minor and rare-earth elements (ppm) in the rocks of the basement complex (1–5) and in the ultrametamorphic rocks developed after them (6–12)

no.	1 (4)	2(14)	3(1)	4(8)	5(5)	6(10)	7(6)	8(6)	9(5)	10(5)	11(9)	12(1)
SiO_2	49.01	68.29	68.65	73.85	71.58	72.28	72.04	74.39	73.46	73.14	74.09	59.81
TiO_2	1.60	0.40	0.62	0.09	0.25	0.21	0.32	0.11	0.03	0.02	0.02	0.16
Al_2O_3	13.93	16.06	13.49	15.13	15.16	14.76	14.25	13.83	14.70	14.54	14.51	21.47
FeO	15.44	3.79	6.01	1.29	2.73	2.20	2.52	1.52	1.09	0.45	0.97	2.16
MnO	0.22	0.06	0.11	0.02	0.05	0.03	0.03	0.03	0.03	0.01	0.04	0.09
MgO	6.31	1.29	2.59	0.42	0.83	0.64	0.57	0.20	0.17	0.11	0.11	0.69
CaO	9.96	3.02	3.10	2.21	2.56	1.92	1.55	0.95	1.10	0.41	0.45	7.80
P_2O_5	0.11	0.09	0.12	0.04	0.06	0.06	0.10	0.03	0.03	0.02	0.09	1.07
K_2O	0.80	1.64	2.30	1.09	1.17	3.11	4.52	4.70	5.48	8.28	4.92	0.84
Na_2O	2.36	4.68	1.92	5.33	4.96	4.24	3.71	3.91	3.44	2.36	4.25	5.08
LOI	0.60	0.45	1.07	0.49	0.82	0.35	0.29	0.65	0.32	0.57	0.52	0.68
Li	19	46	40	5	20	19	29	9	3	2	11	18
Rb	41	78	100	24	49	87	161	184	139	170	295	32
Cs	1.03	2.28	5.00	0.28	2.53	2.29	3.67	3.20	2.50	1.00	11.38	2.00
Ba	154	330	540	163	273	467	665	352	826	1200	115	280
Sr	139	372	170	306	350	343	253	110	209	215	59	370
B	33	6		14	3	20	6	10	5	1	33	
Be	0.65	0.88		1.16	2.42	1.15	0.90	0.75	0.60	0.30	1.08	
F	1400	595		160	190	210	250	120	127	73	158	
Mo	9.60	0.77		0.66	0.78	1.93	0.20	0.60	0.85	2.60	1.47	
Sn	3.20	2.07		0.66	1.14	1.80	2.90	2.55	2.80	0.90	1.27	
La	6.6	23.3		9.4	31.3	9.7	42	3.3	2	2	7	25
Ce	17	40.5		16.07	65.4	14.5	57	9.5			12	58
Nd	13.35	13.8		5.7	12.9	8	34	3.3	2		6.3	29
Yb	5.65	0.77		0.28	0.42	0.63	2.00	0.36	1.80		1.08	4.10
Y	26	5		2	4	2	22	2	8	0	9	46
Zr	96	146		78	118	98	225	121	43	34	37	10
Hf	3.90	3.35		1.43	4.20	4.20		2.50		2.30	1.10	0.20
Ta		0.15		0.55	0.33	0.30		0.45			0.15	0.20
Nb	4.00	4.24		1.28	2.13	6.00		4.10	2.00	1.20	2.45	0.50
Zn	220	57		22	47	35	45	20	20	5	13	
Pb	6	7		10	9	13	27	21	73	89	72	
Cu	120	27		14	35	16	14	3	10	7	29	
Cr	180	19		6	7	8	7	6	11		7	
V	280	52		15	30	8	13	4	3		7	
Ni	80	13		5	5	7	6	4	5		4	
Co	53	9		4	5	4	5	2	2		3	
Sc	42	7		2	5	2	3				1	
Ag	0.01	0.017		0.017	0.025	0.01	0.04		0.09	0.01	0.03	

Note: 1) amphibolite; 2) biotite plagiogneiss with amphibole; 3) biotite plagiogneiss; 4) trondjemite of type 1; 5) trondjemite of type 2; 6) plagioclase–K-feldspar migmatite; 7) K-feldspar migmatite; 8) leucocratic autochthonous granite; 9) pegmatoid paraautochthonous granite; 10) allochthonous granite-pegmatite; 11) K-feldspar and plagioclase pegmatite; 12) pegmatoid plagioclasite. The primary rocks were basalt for (1), plagiogneiss (tonalite) for (2, 4–6) and (8–10), pelite for (3), gneiss and amphibolite for (7), and migmatite and granite for (11, 12).

The rocks of the ultrametamorphic phase show both a positive and a negative Eu anomaly (Figure 3). The age of the K-feldspar migmatites and granitoids in the basement and in the Onot greenstone belt was found to be 2.237 Ga [*Sandimirova et al.,* 1993].

The rocks of the Onot greenstone belt, metamorphosed in the conditions of the amphibolite and epidote–amphibolite facies, occur as a belt, pinching out in places, solely in the rocks of the tonalite–trondjemite association in the Baikal granulite–gneiss region (Figure 1). The belt coincides with the boundaries of the Onot Graben [*Shames,* 1962]. The rocks of the belt are locally covered by the high-grade metamorphic rocks of the Kitoi Series.

The rocks of the belt were classified into (upward) the Burukhtui, Maloiret, Kamchadal, and Sosnovyi Baits suites (Figure 2). The Burukhtui Suite includes apobasaltoid amphibolites, amphibole–biotite schists, quartzites, aporhy-

Table 4. Chemical compositions (wt.%) and the contents of minor and rare-earth elements (ppm) in the rocks of the metamorphic stage of the Onot greenstone belt

no.	1(2)	2(13)	3(4)	4(2)	5(2)	6(2)	7(4)	8(3)	9(10)	10(1)	11(16)
SiO_2	54.50	49.37	75.43	68.08	54.85	90.42	44.02	43.77	0.83	1.00	1.61
TiO_2	0.83	0.96	0.34	0.52	0.71	0.09	0.02	0.02	0.03		0.01
Al_2O_3	11.66	14.48	10.92	14.63	16.11	1.94	0.18	0.86	0.10	0.05	0.08
FeO	12.40	13.02	4.49	5.00	14.81	1.91	54.71	55.96	0.79	1.57	1.18
MnO	0.22	0.20	0.08	0.07	0.10	0.03	0.03	0.01	0.29	0.49	0.25
MgO	8.23	7.66	0.36	1.77	5.26	1.43	1.65	0.37	20.99	20.30	45.56
CaO	8.37	10.09	1.03	2.23	3.02	1.38	0.50	0.20	30.47	29.60	0.90
P_2O_5	0.09	0.08	0.05	0.11	0.09	0.02	0.05	0.09	0.01	0.01	0.01
K_2O	0.51	0.73	3.75	2.85	2.15	0.41	0.04	0.05	0.02	0.03	0.01
Na_2O	2.63	2.45	2.80	3.83	0.56	0.27	0.11	0.11	0.02	0.03	0.01
LOI	0.49	1.00	0.52	0.77	2.46	3.56	1.02	0.53	46.49	46.25	50.4
Li	5	8	5	25	33	2	0	3	tr		
Rb	16	18	119	120	83	22	2	2	tr		1
Cs	0.5	0.6	6.4	2.0	5.0	tr	tr		tr		
Ba	110	125	785	1210	385	18	24	26	13	20	9
Sr	138	121	107	225	108	23	10	12	22	23	5
B	1	13	16	23	6	5	11	22	4	1	4
Be	1.60	0.50	1.90	1.70	1.80	0.10	1.05	1.03	0.18	0.15	0.26
F	650	739	375	630	360	100	243	143	134	110	291
Mo	0.40	0.80	2.00	0.75	0.10	1.00	1.00		0.15	0.10	0.23
Sn	1.40	1.71	4.90	2.35	2.70	0.80	5.30	8.10	0.76	1.10	0.25
La	24	7	79	87	31	16			2	2	2
Ce	33	5	123	141	52	30			2.5	2	2
Nd	17	4	63	60	24	15			2	2	2
Yb	1.90	3.33	7.35	3.60	2.70	0.70	0.20		0.15	0.10	0.30
Y	20	27	68	28	28	2	1		1	0.7	7
Zr	127	101	377	265	123	68	8	31	11	5	5
Zn	109	168	166	60	74	5	54	52	5	5	7
Pb	14	5	20	18	3	2	0	1	1	0	0
Cu	34	146	78	28	6	9	20	7	2	2	3
Cr	725	263	7	76	190	6	2	1	1	1	2
V	246	403	13	62	110	2	12	51	9	11	10
Ni	208	260	6	38	96	3	9	12	3	3	1
Co	33	48	4	16	29	2	11	11	2	3	0.5
Sc	32	124	7	11	22		3		3	1	
Ag	0.01	0.032	0.02	0.025	0.01		0.057				
Au		0.01		0.01			0.04				

Note: 1) amphibolite (metabasaltic andesite); 2) amphibolite (metabasalt); 3) gneiss with biotite, garnet, and amphibole (metarhyolite); 4) garnet–biotite plagiogneiss (metadacite); 5) biotite–garnet plagiogneiss (metapelite); 6) quartzite; 7) magnetite quartzite; 8) hematite quartzite; 9–10) dolomite marble; 11) magnesite marble. The samples were collected from the rocks of the following suites: Maloiret (1); Kamchadal, Burukhtui, and Sosnovyi Baits (2, 4, 6, 9); Burukhtui and Maloiret (3); Kamchadal and Sosnovyi Baits (5), Kamchadal (7, 10, 11), and Sosnovyi Baits (8).

olite and apopelite garnet–biotite plagiogneisses and plagioschists, quartzites, and marmorized limestones. The Maloiret Suite includes aporhyolite and apodacite biotite and biotite–garnet plagiogneisses, apopellite amphibole–biotite (locally with garnet) and biotite microgneisses, and apobasaltic andesite amphibolites. The Kamchadal Suite includes marbles, in which a magnesite variety dominates over the dolomite and calcite varieties. The marble beds are interstratified with amphibolites, monomineral and iron quartzites, amphibole, garnet–amphibole, biotite and garnet–biotite schists, and gneisses. The Sosnovyi Baits Suite is dominated by amphibolites and biotite–garnet gneisses, which are thinly (in a flyschlike manner) interlayered by hematite–magnetite, hematite, monomineral, and sillimanite quartzites. The compositions of the rocks of the metamorphic phase are presented in Table 4, and their REE distribution patterns, in Figure 3b. A series of isochrons with ages ranging between 2.675±0.095 Ga with $(^{87}Sr/^{86}Sr)_0 = 0.701$ and 2.786±0.059 Ga with $(^{87}Sr/^{86}Sr)_0 = 0.702$ was derived by a Rb–Sr method using amphibolites (metabasaltoids) and biotite–garnet gneisses (metarhyolites) of different suites.

Table 5. Chemical compositions (wt.%) and the contents of minor and rare-earth elements (ppm) in the rocks of the ultrametamorphic stage of the Onot greenstone belt

no.	1 (2)	2 (2)	3 (5)	4 (1)	5 (1)	6 (1)	7 (1)	8 (2)	9 (2)	10 (3)
SiO_2	72.39	70.27	75.53	59.18	67.64	49.33	41.50	42.47	50.27	49.37
TiO_2	0.24	0.31	0.04	1.30	0.02	0.55	0.15	0.03	0.06	1.90
Al_2O_3	14.16	15.01	13.54	13.77	0.38	10.85	4.99	0.98	0.49	13.83
FeO	2.64	2.78	1.02	12.24	29.05	32.58	40.47	57.23	2.93	16.53
MnO	0.04	0.04	0.02	0.16	0.13	0.21	0.28	0.01	0.62	0.24
MgO	0.67	1.03	0.23	3.24	1.25	4.25	6.41	2.40	16.40	5.65
CaO	1.62	1.42	0.85	4.84	1.04	3.09	7.77	1.56	23.75	9.20
P_2O_5	0.04	0.10	0.03	0.14	0.02	0.02	0.03	0.03	0.01	0.21
K_2O	3.28	4.46	4.34	1.51	0.02	0.04	0.05	0.06	0.14	0.52
Na_2O	4.46	3.47	3.50	2.38	0.01	0.24	0.76	0.28	0.06	1.93
LOI	0.44	0.71	0.46	1.36	0.38	0.24	0.96	0.22	5.50	1.01
Li	16	17	3	6	2	2	2		8.5	7
Rb	103	130	171	130			4	2	2	8
Cs	3	2.5	4.25	22						1
Ba	515	930	248	360	20	5	120	27	33	167
Sr	86	330	106	120	5	60	20	17	25	117
B	6	22	12	36	10	10	8	16	10	4
Be	1.3	2	0.3	6.3	0.5	0.5	1.95	1.6	0.12	0.5
F	440	470	130	500			200	120	230	
Mo	0.5	2.4	1.8	1	2	0.2	0.5	0.5	0.5	2.5
Sn	4.05	3.9	2.2	28	1	0.6	0.5	0.2	3.2	4.5
La		43	31	30		5			4	5
Ce		80	48	60					5	
Nd		30	16	29					4	
Yb		0.9	0.39	2	0.5	1			0.25	1.5
Y		6	4	26	3	15			2	20
Zr	97	185	59	150	10	80	22	12	15	127
Zn	53	33	5	280	100	200	170	150	37	250
Pb	29	51	30	24	1	1	0	0	14	13
Cu	5	37	11	13	50	8	520	9	3	128
Cr	7	1	8	35	5	200	69	1	6	80
V	9	30	7	250	5	100	66	11	15	225
Ni	4	10	6	65	10	300	23	11	4	120
Co	4	2	1	45	4	20	90	5	12	50
Sc				28	1	30				20
Ag	0.01		0.02	0.05						0.01

Note: 1) schlieric biotite plagiomigmatite; 2) K-feldspar migmatite; 3) leucocratic granite; 4) garnet–quartz–amphibole rock; 5) pyroxene–magnetite rock; 6) ferrosilite–amphibole–quartz–garnet rock; 7) cummingtonite–magnetite rock; 8) ferrosilite rock; 9) pyroxene skarn; 10) garnet–amphibole rock with biotite. The primary rocks were amphibolite for (1, 10), gneiss and amphibolite for (2, 3), iron quartzite for (4–8), and dolomite marble for (9).

The rocks of the ultrametamorphic stage contain relicts of the metamorphic rocks and are represented by plagiomigmatites, K-feldspar and schlieric K-feldspar migmatites, granites, and also by garnet–amphibole biotite-bearing basic rocks in the gneisses and amphibolites; by pyroxene skarns in the dolomite marble, and by skarns with enstatite, forsterite, and spinel in the magnesite marble; and by garnet–quartz–amphibole, pyroxene–magnetite, ferrisilite–amphibole–quartz–garnet, cummingtonite–magnetite, and ferrisilite metasomatic rocks in the iron quartzites. The chemical compositions of these rocks are given in Table 5. The ultrametamorphic rocks developed after the alumosilicate rocks are enriched in SiO_2, K_2O, Na_2O, Rb, Cs, Ba, Sr, B, Mo, Sn, light REE, Zr, Pb, Ag, and Au, and are depleted in iron, CaO, MgO, F, Yb, Y, Zn, Cu, Cr, V, Ni, Co, and Sc.

The replacement of the dolomite and magnesite marbles by skarn increased the contents of SiO_2, Al_2O_3, iron, alkalis, and most of trace elements and diminished CaO and (or) MgO. The iron quarzites show the removal of SiO_2 and iron and the concentration of Al_2O_3, CaO, MgO, alkalies, and most of the trace elements (Tables 4 and 5; Figure 3b).

The rocks of the post-ultrametamorphic phase are developed in the basement complex and in the greenstone belt. They occur as elongated lenticular bodies, ovals, sheets, and pockets and have a distinct or poorly expressed zonal struc-

Table 6. Chemical compositions (wt.%) and the contents of minor and rare-earth elements (ppm) in the rocks of the post ultrametamorphic stage of the Kitoi Series and the Onot and Arban complexes

no.	1(8)	2(15)	3(1)	4(1)	5(10)	6(5)	7(3)	8(1)	9(11)	10(1)	11(6)	12(1)	13(1)	14(2)
SiO_2	51.77	49.36	56.50	60.82	49.15	48.62	52.18	73.15	57.75	57.48	56.38	43.40	79.67	30.19
TiO_2	1.36	1.38	1.19	1.10	0.91	0.86	1.31	0.58	0.93	1.13	0.42	0.11	0.36	0.35
Al_2O_3	13.64	15.37	14.17	10.16	14.15	14.89	15.46	10.41	18.52	18.03	17.11	20.57	9.91	7.51
FeO	14.64	13.47	11.25	21.28	12.36	11.28	16.12	6.90	10.76	5.51	9.09	4.02	3.15	7.01
MnO	0.20	0.20	0.13	0.19	0.20	0.15	0.17	0.07	0.15	0.07	0.15	0.11	0.02	0.64
MgO	5.75	6.24	3.88	3.83	7.75	10.08	6.48	2.46	4.20	5.59	3.89	0.86	0.59	2.21
CaO	8.30	9.50	7.20	1.57	10.75	4.82	2.92	1.91	1.37	1.29	6.51	18.41	0.50	28.14
P_2O_5	0.15	0.12	0.15	0.12	0.08	0.06	0.09	0.07	0.08	0.32	0.12	0.22	0.08	0.05
K_2O	1.20	0.92	1.73	0.33	1.13	1.33	1.47	1.32	2.97	4.41	2.37	1.88	3.48	1.34
Na_2O	2.79	2.41	2.35	0.03	1.81	1.50	1.93	1.67	1.67	2.34	1.67	2.69	1.40	0.42
LOI	1.231	1.248	1.51	0.58	1.746	1.97	1.61	1.39	2.00	3.77	2.295	7.74	0.76	21.37
Li	12	5	13	14	6	12	34	9	20	60	29	12	15	16
Rb	26	23	42	18	24	31	59	31	78	210	54	58	96	31
Cs	0.58	0.55	0.10	2.00	0.10	0.55	3.28	0.10	5.17	2.00	6.00		2.00	0.10
Ba	276	195	390	100	187	331	344	295	573	820	478	310	770	265
Sr	167	187	400	20	116	159	95	95	109	320	203	280	140	95
B	14	13	5	95	30	45	26	1	84	22	25	23		4
Be	2.08	1.26		0.40	1.50	0.45	0.83	3.00	2.74	1.65	1.30	1.90		
F	1508	925		375		255	590		760	2600	590	500		
Mo	5.75	0.53		2.20	0.50	0.60	0.50	3.00	2.87	0.30	0.35	0.50		
Sn	3.72	2.03	2.00	3.40	0.30	2.40	2.53	2.00	3.94	2.20	3.50	2.00		1.00
La	33	16		5	15	2	4	20	37	65	30	4		
Ce	50	35		5	30	6	13	50	73	140	70	20		
Nd	28	13		5		5	9		29	54	40	10		
Yb	3.86	3.47		3.20	3.00	1.97	3.50	2.00	2.13	2.00	2.20	1.60		
Y	28	33		28	30	19	30	20	26	20	21	15		
Zr	131	95	150	110	55	73	114	150	139	170	110	14	140	115
Zn	168	145	80	250	200	97	158	100	164	75	100	36		35
Pb	9	5	6	10	3	9	9	15	24	4	14	9		10
Cu	90	93	100	29	150	141	110	80	68	24	48	11		15
Cr	105	121	5	100	160	454	101	200	322	240	275	22		125
V	347	307	200	200	335	210	200	100	142	150	104	170		20
Ni	73	78	40	80	120	128	120	100	101	110	66	17		40
Co	50	41	40	40	47	51	50	15	27	34	28	14		40
Sc	45	55			42	38		15	43	26				
Ag	14.05	0.03	0.10			0.03	0.06		0.06	0.01				0.06
Pd		0.006			0.006			0.05	0.006					0.001

Note: 1–2) and 5–6) are amphibole rocks; 3) biotite–amphibole rock; 4) amphibole–garnet–quartz rock; 7) biotite–plagioclase–garnet–amphibole rock; 8) garnet–biotite–plagioclase–quartz rock; 9) substantially biotite rock with staurolite, garnet, amphibole, and plagioclase; 10) quartz–plagioclase–amphibole rock with muscovite; 11) garnet–plagioclase–staurolite–biotite–quartz rock; 12) zoisite–epidote–amphibole–plagioclase rock; 13) muscovite–biotite–plagioclase–quartz rock; 14) carbonate-bearing rock with garnet, biotite, and amphibole. The rock samples were collected from the following suites: Kitoi (1), Kamchadal Suite and the basement (2), Kamchadal (3, 8–12, 14), Sosnovyi Baits (4, 6, 7), Arban (5), and the basement (13). The primary rocks were gabbro–anorthosite for (1), gabbro and basic schist for (2), schist for (3), amphibolite for (4, 7–9, 14), gabbro for (5–6), granite for (10), gneiss for (11), amphibolite for (12), and tonalite for (13).

ture. Their characteristic feature is the areally spread scatter of minerals as disseminated particles. The most widely developed are apogabbro and schistose amphibole, biotite–amphibole, amphibole–garnet–quartz, biotite–plagioclase–garnet–amphibole, quartz–garnet–biotite–plagioclase-quartz and quartz–garnet (often with disthene), substantially biotite (with staurolite, garnet, amphibole, and plagioclase), quartz-plagioclase-amphibole, apodolomite quartz-hematite-amphibole–graphite, apogneiss garnet–plagioclase–staurolite–disthene–biotite–quartz, zoisite–epidote–amphibole–plagioclase, muscovite–biotite–plagioclase–quartz, and carbonate–bearing (with garnet, chlorite, and amphibole) metasomatic rocks. Some of them are of the high-pressure kyanite–sillimonite type. The specific features of their composition are the elevated, relative to the source material, contents of K_2O, MnO, Li, B, Be, Sn, Mo, F, Zr, Ag, Au, and Pd (Table 6). The post-ultrametamorphic biotite–garnet–quartz–plagioclase metasomatites with silimonite,

Table 7. Chemical compositions (wt.%) and the contents of minor and rare-earth elements (ppm) in the gabbroids, metaultrabasics, and granitoids

no.	1 (9)	2 (2)	3 (27)	4 (14)	5 (21)	6 (9)
SiO_2	48.60	45.14	68.24	73.73	73.93	74.09
TiO_2	1.35	0.45	0.83	0.40	0.25	0.02
Al_2O_3	13.70	4.14	13.42	12.65	12.88	14.51
FeO	14.01	13.56	5.30	2.89	2.52	0.97
MnO	0.21	0.18	0.07	0.04	0.04	0.04
MgO	7.47	28.77	0.97	0.40	0.37	0.11
CaO	11.08	4.94	2.43	1.21	0.92	0.45
P_2O_5	0.11	0.05	0.27	0.07	0.06	0.09
K_2O	0.55	0.05	4.53	5.30	5.62	4.92
Na_2O	2.09	0.23	2.98	2.82	2.91	4.25
LOI	0.96	0.79	0.70	0.5	0.31	0.52
Li	7	2	15	8	5	11
Rb	13	1	138	171	183	295
Cs	0.3	0.1	1.9	2.0	2.4	11.4
Ba	149	75	1488	997	732	115
Sr	123	88	279	170	139	59
B	14		8	7	11	33
Be	0.69		2.06	1.95	1.88	1.08
F	463		1100	666	303	158
Mo	0.73		1.70	1.11	1.10	1.47
Sn	1.80		5.38	6.19	7.13	1.27
La	16		100	76	39	7
Ce	43		131	111	65	12
Nd	27		77	48	33	6
Yb	2.22		3.83	5.52	4.33	1.08
Y	21		35	45	32	9
Zr	64	43	328	304	238	37
Hf	1.60		10.32	7.75	5.47	1.10
Ta	0.10		1.10	1.15	4.05	0.15
Nb	1.55	9.00	10.74	15.40	26.47	2.45
Zn	173		76	43	47	13
Pb	3		32	28	37	72
Cu	138		10	6	9	29
Cr	206		15	9	8	7
V	314		59	31	15	7
Ni	107		9	6	4	4
Co	47		6	5	4	3
Sc	25		15	7	9	1
Ag	0.05		0.02	0.10	0.02	0.03

Note: 1) gabbro of the Arban Complex; 2) metaultrabasic rock of the Ilchir Complex; 3–6) granitoids of the Shumikha Complex: biotite–amphibole granodiorite of phase 1 (3), leucocratic granite of phase 2 with biotite and amphibole (4), granite- and granosyenite porphyry and aplite-like granite of phase 3 (5), and K-feldspar and plagioclase pegmatite (6).

staurolite, and muscovite yielded isochrons ranging between 1.994±0.012 Ga with $(^{87}Sr/^{86}Sr)_0 = 0.709\pm0.0007$ and 2.117±0.0145 Ga with $(^{87}Sr/^{86}Sr)_0 = 0.717\pm0.0008$. It appears that the formation of high-pressure rocks in the Arban Massif [*Sharkov et al.,* 1996] should be dated by the same period of time.

Arban gabbroids and Ilchir metaultramafics occur as a number of massifs, ranging from a few to hundreds of meters (rarely tens of kilometers), localized in the rocks of the basement, of the Kitoi Series, and of all suites of the Onot greenstone belt. The chemical compositions of these rocks are given in Table 7 (columns 1 and 2). The fact that these gabbroids and ultramafics were not involved in the ultrametamorphic transformations, but were actively replaced by the postultrametamorphic rocks suggests that their formation might have taken place in the time interval of 2.18–2.2 Ga.

Shumikha granitoid complex is definitely restricted to a zone of junction of the highly metamorphozed rocks of the Sharyzhalgai and Kitoi series with the rocks of the Onot greenstone belt and is traceable both in them and also in the gray gneisses of the basement over a distance of 250–300 km (Figure 1). As an independent complex, these granitoids were mapped during the geological surveys of the Irkutskgeologiya Association conducted in the last decade. Earlier, most of these rocks had been included into the Sayan Complex. The rocks occur as one- or multiphase plutons ranging from tens of meters to 10–15 km in size. The rocks of the first phase are massive and porphyry-like amphibole, amphibole–biotite, and biotite granodiorites (often with hypersthene). The rocks of the second phase are massive biotite granites, and those of the late phases are vein aplite, granodiorite-, granosyenite-, and granite porphyry, and leucogranites. The compositions of these rocks are listed in Table 7 (columns 4–6), and their REE distribution patterns are displayed in Figure 3d.

The time of the granitoid formation determined by a Rb-Sr method for the amphibole and amphibole–biotite granodiorites and granite porphyry of the Onot Massif was found to be 1.983±0.048 Ga with $(^{87}Sr/^{86}Sr)_0$ = 070633±0.00045. Similar granites, attributed to the Sayan Complex (Barbitai Massif in the NW Sayan region), were dated by a U-Pb method using zircons and found to be 1.848±0.018 Ga old with MSWD = 6.6 [*Kirnozova et al.,* 2000].

Pegmatites and granite pegmatites are widely developed in the rocks of the Kitoi Series and gray-gneiss complex and are much more rare in the belt itself. They do not show any clearly expressed zoning. They are dominated by plagioclase and K-feldspar varieties with tourmaline (schorl), garnet, muscovite, and orthite (Table 7, column 6). The K-feldspar varieties were found to be abnormally high in Li, Rb, and Cs. These rocks were dated 1.86±0.004 Ga with $(^{87}Sr/^{86}Sr)_0$ = 0.738±0.0003.

The metasomatites of deep fault zones are restricted to the zones of the Dabad (Kitoi–Zalari), Alagni–Kholomkha (Savinskii), Onot–Khartagninskii, and other faults. The alumosilicate rocks are dominated by albite, quartz–microcline–chlorite (with biotite, muscovite, and amphibole), and chlorite or serpentine–chlorite rocks; the early skarn and magnesite marble are dominated by talc-bearing associations. Much rare are low-temperature metasomatites with amphibole, K-feldspar, and biotite. The compositions of these rocks are listed in Table 8 and were discussed earlier [*Levitskii,* 1994]. The age of the rocks is 633±7 Ga with $(^{87}Sr/^{86}Sr)_0$ = 1.2255±0.0063.

Discussion of Results

The geochronological, geological, and petrological data suggest the following sequence of the rock formation: the tonalites, trondjemites, and amphibolites of the basement—the granulite-facies metamorphic rocks of the Kitoi Series—the rocks of the Onot greenstone belt—the ultrametamorphic rocks—the gabbroids of the Arban Complex—the rocks of the post-ultrametamorphic phase—the metasomatic rocks of the deep fault zones. As a rule, the rocks have tectonic contacts which host abundant metasomatic rocks of various types. The main structural, petrographic, isotopic, and geochronological characteristics of the rocks are summarized in Table 9. The rocks have their own distinct fields in the AFM diagram of Figure 4.

As follows from their petrogeochemical, geochronological and isotopic characteristics, the rocks of the tonalite–trondjemite composition are similar to the trondjemite gneisses of Amitsok and Nuk, Greenland [*Mac-Gregor,* 1983], to the low-K gneisses of Swaziland and the tonalites of the Tispruit Pluton, South African Republic [*Collerson and Bridgewater,* 1983], and to the Waiwak-1 tonalite–trondjemite gneisses of Labrador, Canada [*Collerson and Bridgewater,* 1983]. Earlier, based on their structural and textural features, mineral composition, their contents of petrogenic and trace elements, their K/Rb, Rb/Sr, Sr/Ba and Ba/Rb ratios, their REE distribution patterns, their positive Eu anomaly (Figure 3a), and also on their abnormally high mantle $^{87}Sr/^{86}Sr$ ratios, *Sandimirova et al.* [1992] and *Nozhkin et al.* [1995] concluded that the rocks of the tonalite–trondjemite composition were similar to the oldest granitoids of the Earth [*Trondjemites, Dacites...,* 1983]. Based on a number of their properties, *Condie and Hanter* [1976], *Hanter* [1983], and *Hanter et al.* [1978] believed them to be most close to the trondjemites of Swaziland and to the trondjemites of the Tispruit diapiric pluton from the Barberton greenstone complex (SAR). Considering the whole set of data, these rocks originated under continental conditions. Earlier, *Petrova and Levitskii* [1984] proved that the initial rocks of the Sharyzhalgai Complex developed SW of Lake Baikal were oceanic formations with an age of 3,1–3.7 Ga [*Gornova and Petrova,* 1999; *Mekhonoshin et al.,* 1987; *Sandimirova et al.,* 1979]. Therefore, it can be assumed that the basement of the marginal part of the Siberian Craton included both Early Archean sialic continental crust and mafic oceanic crust, both having low (0.700–0.701) primary $^{87}Sr/^{86}Sr$ ratios and similar ages (3.1–3.7 Ga), the age of the high- and low-grade metamorphic protolith (Table 9).

The mineral composition and petrogeochemical properties of the rocks of the Kitoi Series, such as the variations and high contents of SiO_2, Al_2O_3, CaO, K_2O, Li, Ba, Rb, B, Zr, Hf, Nb, Cr, and Ni (Table 1), as well as the high $(^{87}Sr/^{86}Sr)_0$ ratios, suggest that a substantial contribution to the composition of the Kitoi rocks was made by the products of the disintegration, weathering, and chemical differentiation of the earlier continental (basement complex) and oceanic (Sharyzhalgai Complex) rocks. The metavolcanics are scarce and belong to a calc-alkalic series (Figure 4, Table 1). The new geochronological and petrogeochemical data justify the interpretation of the Kitoi Series as an independent stratigraphic unit of the Sharyzhalgai Complex.

The rocks of the Onot Belt accumulated in a paleorift, where bimodal volcanic rocks, with a growing amount of basaltoids and tuff, were succeeded first by terrigenous (clastic) sediments and then by chemogenic carbonate (both lagoonal and deep-sea) sediments. The volcanic rocks vary from basalts to rhyolites (Table 4; Figure 3b). The existence of one mantle source, which controlled the mechanism of petrogenesis during a long period of time, is proved by the low $(^{87}Sr/^{86}Sr)_0$ values obtained for the basement rocks

Table 8. Chemical compositions (wt.%) and the contents of minor and rare-earth elements (ppm) of metasomatic rocks from deep-fault zones

no.	1(5)	2(2)	3(4)	4(1)	5(3)	6(11)	7(12)	8(1)	9(1)	10(11)	11(18)	12(3)	13(1)
SiO_2	72.16	58.30	61.67	53.93	36.70	34.57	45.90	46.30	36.42	20.88	59.61	51.58	42.98
TiO_2	0.18	1.09	0.16	0.87	1.06	0.01	0.23	0.01	1.97	0.14	0.02	0.02	0.01
Al_2O_3	14.41	17.09	18.21	18.43	17.17	0.36	6.94	0.07	14.29	3.35	0.45	0.30	0.47
FeO	1.57	6.22	2.05	9.28	7.54	0.76	3.27	1.49	3.36	9.73	1.05	0.89	1.40
MnO	0.01	0.07	0.02	0.09	0.08	0.05	0.07	0.10	0.02	0.21	0.05	0.07	0.03
MgO	0.51	5.39	8.36	3.91	25.83	26.44	25.55	35.62	32.09	29.46	30.82	10.90	40.80
CaO	0.42	1.59	0.19	3.45	0.21	20.01	2.86	0.31	0.14	5.98	1.25	14.29	0.06
P_2O_5	0.07	0.44	0.09	0.14	0.06	0.01	0.04		0.05	0.03	0.02	0.01	0.03
K_2O	7.49	3.48	3.74	1.66	0.70	0.03	0.67	0.01	0.02	0.04	0.02	0.06	0.01
Na_2O	2.32	2.66	0.02	6.48	0.08	0.08	0.02	0.02	0.32	0.09	0.05	0.11	0.32
LOI	0.763	3.65	5.53	1.77	10.61	17.83	13.86	16.1	11.36	29.89	6.75	20.68	13.93
Li	4	57	23	14	57	5	23	2	91	16	4	10	2
Rb	355	160	55	90	21	1	15			2	2		
Cs	4.25	2.00	3.25	7.00	1.75	0.38	1.05			1.00			
Ba	818	920	47	190	27	38	25	22	23	14	20	10	
Sr	145	360	17	120	8	55	9	5	5	9	8	15	
B	10	25	58		28	134	15	26	16	5	8	6	
Be	1.85	2.15	1.84		1.18	0.25	0.81	0.05	2.40	0.86	0.22	0.42	
F	338	2000	518		472	472	542	280	500	353	817	300	
Mo	0.30	0.30	0.50		0.69	0.55	0.47			0.65	0.73		
Sn	44.13	3.20	1.45		2.35	0.78	1.30	0.50	3.10	2.42	0.69	0.75	
La	12	100	3		19	2	7		12		3	5	
Ce	32	180			41	2							
Nd	11	67			12	2	5		19				
Yb	1.58	2.10	5.30		2.51	0.13	0.87		3.80		7.00	7.40	
Y	12.5	23	47		13.6	0.37	10.42		35		37	48	
Zr	141	190	46	160	55	6	30	5	120	59	6	5	
Zn	9	73	16		67	18	27	5	5	47	5	5	
Pb	22	8	2		0	5	0	0	0	3	2	0	
Cu	526	20	2		10	3	4	3	1	37513	2	4	
Cr	13	180	3		217	2	61	1	22	34	5	1	
V	13	150	16		251	8	43	2	360	58	3	12	
Ni	7	110	6		138	8	34	1	22	32	11	2	
Co	2	25	7		43	2	8	1	16	94	4	0	
Ag	3.23					0.26				0.03			
Au					0.01					0.004			
Pd					0.001					0.009			

Note: 1) albite–quartz–microcline rock with muscovite and chlorite; 2) chlorite–muscovite rock; 3) chlorite–quartz–sericite rock; 4) epidote–plagioclase–quartz rock; 5) chlorite rock with serpentine, sericite, and talc; 6) serpentine rock (ophicalcite); 7) chlorite–serpentine–talc rock with quartz; 8) talc–serpentine rock; 9) hematite–chlorite–talc rock; 10) sulfide-bearing rock; 11) substantially talc rock; 12) quartz–dolomite rock; 13) asbestos rock. The primary rocks were granite for (1–4); granite, amphibolite, and migmatite for (5); dolomite marble for (6); apomagnesite skarn for (7); magnesite marble for (8); schist for (9); gneiss, schist, and marble and metasomatic rocks after them (10); magnesite marble and magnesian skarn for (11); serpentine rock for (12). The suites involved were Kamchadal (1–5 and 7–13) and Burukhtui (6).

and for the apobasalt amphibolites and aporhyolite garnet–biotite gneisses (Table 9). This fact justifies the interpretation of the granite–greenstone regions as independent and most important structural elements in the structure of the Precambrian continental crust.

The facts of the destruction of the early rocks and the profound differentiation of the weathering products are proved by the presence of marbles and monomineral iron and alumina quartzites produced by the accumulation of SiO_2, Fe, MnO, CaO, MgO, and trace elements (Table 5). The common chemogenic conditions of carbonate formation are indicated by the absence of SiO_2 and Al_2O_3 in the dolomite, magnesite, and calcite marbles and by the elevated contents of MnO and iron in the rocks of the Onot Belt and the Kitoi Series (Table 1, column 4; Table 4, columns 9–12). These and other data suggest that the rocks of the Kitoi Series accumulated as a result of the area disintegration and weathering of rocks under terrigenous–chemogenic conditions, and

Table 9. Rock-structural and isotope-geochronological characteristics of rocks that originated successively in the SW Baikal and SE Sayan regions

Rock-structural type	Series, complex	Method of study and site	Sample material	Age, Ga	$^{87}Sr/^{86}Sr$	Reference
Baikal granulite-gneiss region	Sharyzhalgai Series	Rb/Sr	Basic two-pyroxene, plagioclase schists; SW coastal area of Lake Baikal, Oringol iron ore district	3.7	0.701	[*Sandimirova et al.*, 1979]
		Rb/Sr		3.49	0.7016	[*Mekhonoshin et al.*, 1987]
		Rb/Sr		3.104	0.7021	[*Gornova and Petrova,* 1999]
	Kitoi Series	Rb/Sr	Plagiogneisses, Onot R. and Biboi R. drainage areas	2.827	0.7055	[*Levitskii et al.*, 1995]
	Sharyzhalgai Series	U/Pb for Zr	Charnockite-series enderbite, plagiogranite, garnet–cordierite and hypersthene migmatites, granite	2.4–2.3; 2.2–2.4; 2.4; 2.5; 1.9		[*Bibikova et al.*, 1990]
		U/Pb for Zr	Charnoenderbite, garnet gneiss; SW coast of L. Baikal	2.46±0.01; 1.96±0.01; 1.75-1,85; 2.85±0.07; 2.78±0.048		[*Aftalion et al.*, 1991]
		Rb/Sr Sm/Nd	Garnet gneiss, migmatites; SW coast of L. Baikal	1.96±0.16; 2.275; 2.42; 2.34		[*Aftalion et al.*, 1991]
East Sayan granite–greenstone region	Rocks of Onot Belt basement	U/Pb for Zr	Plagiogneiss granite; Onot R.	3.25		[*Bibikova et al.*, 1982]
		Rb/Sr	Trondjemite; Onot, Savina, and M. Belaya rivers	3.711	0.6984± 0.0015	[*Sandimirova et al.*, 1992]
		Rb/Sr	Trondjemite and tonalite; Onot and M. Belaya rivers	3.113± 0.039	0.7004± 0.0005	Our data (in press)
	Onot Belt, Maloiret and Kamchadal suites	Rb/Sr	Apobasalt amphibolite, aporhyolite biotite–garnet gneiss; Onot R.	2.675 2.786	0.7016 0.7018	[*Levitskii et al.*, 1995]

those of the Onot Belt accumulated as a result of extensive redeposition only in synform linear zones in the same period of time.

The evolution of the metabasaltic rocks from the early associations in the tonalite–trondjemite basement, the Kitoi Series, and the lower levels of the Onot greenstone belt (lower levels of the Maloiret Suite) to the upper levels of the Kamchadal Suite is imprinted in the replacement of the

Table 9. (continued)

Rock-structural type	Series, complex	Method of study and site	Sample material	Age, Ga	$^{87}Sr/^{86}Sr$	Reference
Rocks of ultrametamorphic stage	Basement Complex, Kitoi Series, Onot greenstone belt	Rb/Sr	Plagiomigmatites, K-feldspar migmatites, granitoids; Onot, Savina, and Malaya Belaya drainage areas	2.237	0.7041	[*Sandimirova et al.,* 1993]
				2.40 2.60	0.704 0.703	[*Levitskii et al.,* 1995]
Rocks of postultrametamorphic tage	Basement Complex, Kitoi Series, Onot Belt, ultrametamorphic rocks	Rb/Sr	Amphibole and garnet–biotite–plagioclase–quartz rocks with staurolite and disthene; Savina, Onot, and M. Belaya drainage basins	1.994 2.128	0.7089 0.7168	[*Levitskii et al.,* 1995]
Blocks of the Sayan marginal basement salient	Shumikha granitoid complex	Rb/Sr	Amphibole and amphibole–biotite granodiorite, aplite, and garnet porphyry; Onot R.	1.983	0.7063	[*Levitskii et al.,* 1995]
	Sayan granitoid complex	U/Pb for zircons	Amphibole–biotite granodiorite with hypersthene; Barbitai R.	1.848		[*Kirnozova et al.,* 2000]
	Pegmatites	Rb/Sr	Plagioclase and K-feldspar pegmatites and granite-pegmatites; Onot R.	1.86	0.738	[*Sandimirova et al.,* 1993]
Deep fault zones	Dabad and Alagna–Kholomkha faults	Rb/Sr	Chlorite rocks or same with serpentine, sericite, and talc; Onot R.	0.633	1.225	[*Sandimirova et al.,* 1993]

calc-alkalic differentiation trend by the dominating tholeiitic trend, close to NMORB (Figure 9). Based on the absence of the contiguous series of basic and ultrabasic rocks and on the presence of basic, intermediate, and acid volcanics, which sometimes occur as bimodal series with comparable $(^{87}Sr/^{86}Sr)_0$ values, the Onot Belt can be classified as a secondary greenstone belt of the calc-alkalic type [*Condie,* 1983], which originated on the early sialic tonalite–trondjemite crust. Its apobasalt and apobasaltic andesite amphibolites from the base of the sequence include varieties similar to the Archean differentiated basalts of the TH2 type with TH1 basalts dominating greatly in the top [*Condie,* 1983]. The metarhyolite and metaandesite gneisses are similar to F2-type gneisses [*Condie,* 1983], characterized by their REE fractionation (Figure 3b). A distinctive feature of the Onot Belt is the presence of carbonate rocks and the predominance of magnesite, known from the Kalar greenstone belt of India [*Monin,* 1987]. It is worth mentioning the fact that the rocks of the lower Maloiret Suite showed an older age (2.786 Ga) than the age of the rocks from the middle and top of the Kamchadal Suite (2.675 Ga), where various types of marble, gneiss, and quartzite dominate over the metavolcanics. This suggests the age and isotopic specifics of this belt's rock accumulation history and calls for more geochronological, geological, and geochemical investigations to prove the accumulation sequence of various suites.

The processes of ultrametamorphism (granitization) were especially active in the junction zone between the East Sayan granite–greenstone and the Baikal granulite–gneiss regions. They facilitated the homogenization of the rocks of the base-

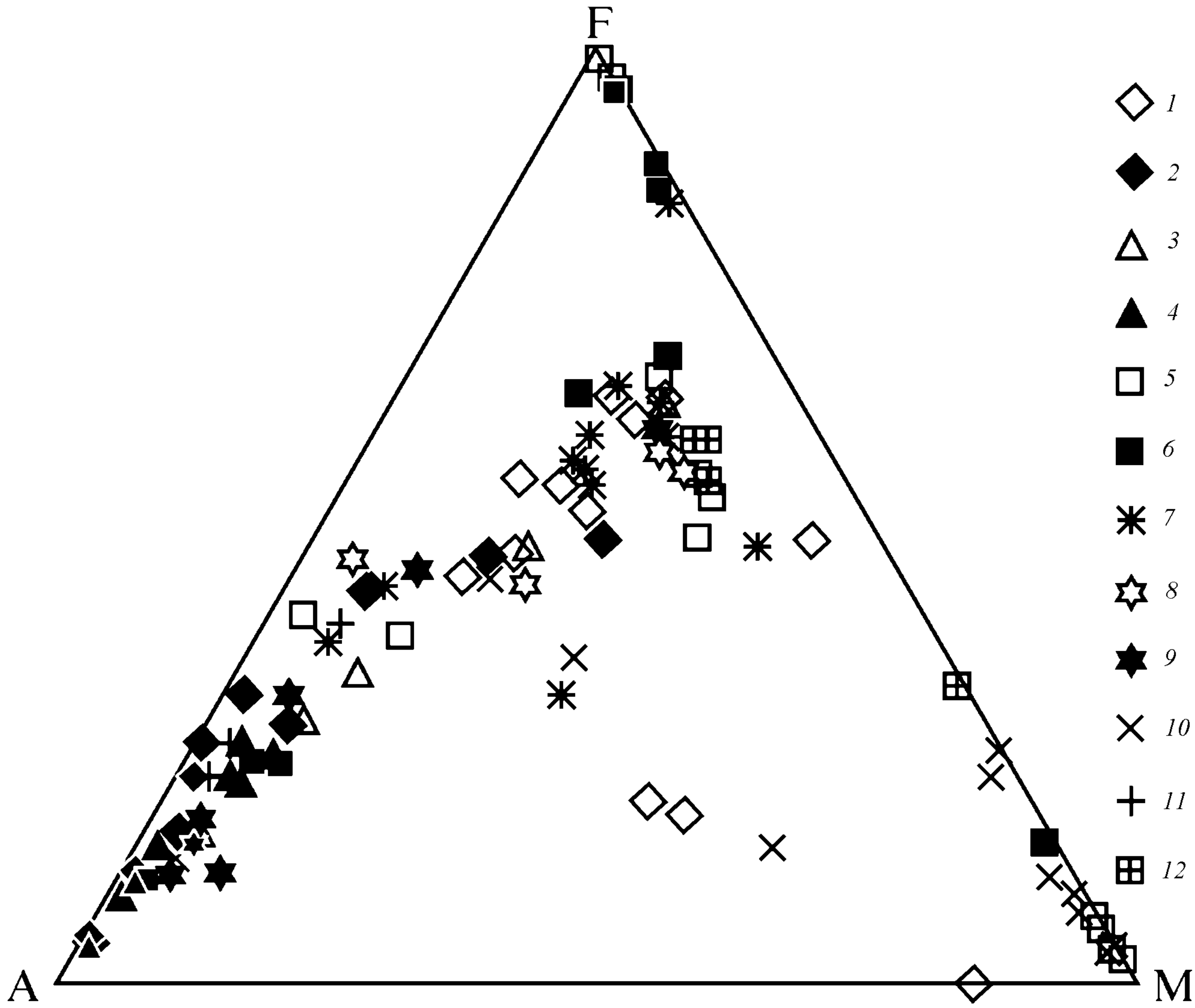

Figure 4. AFM diagram for the mean compositions of rocks.
(1–2) rocks of the Kitoi Series of the metamorphic (1) and ultrametamorphic (2) stages; (3–4) rocks of the basement complex of the metamorphic (3) and ultrametamorphic (4) stages; (5–7) rocks of the Onot greenstone belt of the metamorphic (5), ultrametamorphic (6), and postultrametamorphic (7) stages; (8–9) rocks of the Targazoi greenstone belt of the metamorphic (8) and ultrametamorphic (9) stages; (10) metasomatic rocks from deep fault zones developed after different primary rocks; (11) granitoids of the Shumikha Complex; (12) rocks of the Arban, Ilchir, and Nerchinsk complexes.

ment, the Kitoi Series, and the Onot greenstone belt, the obliteration of contacts between them, and the formation of one granite–metamorphic layer of the Earth's crust, in which its high- or low-metamorphic substrate can be distinguished in very rare cases. At the early stages these processes were marked in the alumosilicate rocks by the formation of various migmatites, at the late stages, by the formation of granites and skarn after the marble. Skarn with spinel, forsterite, and enstatite was formed after the magnesite. In its turn, this skarn served as a source rock for the formation of commercial talcite deposits. The iron quartzite served as a source material for producing metasomatites with garnet, ortho- and clinopyroxene, amphibole, and quartz. In all cases one can trace the superimposed character of transformations over all types of rocks and the effect of the source rocks on the compositions of the newly formed materials. The result of these processes was the fact that the rocks of the ultrametamorphic phase, developed after the amphibolites (on a moderate scale) and after the high-Al gneisses, are higher in SiO_2, K_2O, Rb, Ba, Zr, Pb, and light REE and lower in Fe, MgO, CaO, and, in some cases, in Na_2O, Li, Be, F, Mo, Sn, Yb, Y, Zn, Cu, Cr, V, Ni, Co, Sc, and Ag, as compared to the source material (Tables 1–6). The migmatites after the tonalite and trondjemite are slightly lower in SiO_2 and Na_2O (Table 3). The metasomatites after iron quartzites are lower in SiO_2 and iron and higher in CaO and MgO. Where skarn developed after the marble, the contents of these elements are lower, but their SiO_2 and Al_2O_3 contents are higher. On the whole, the rocks of the ultrametamorphic phase showed, compared to the source material, the accumulation of light REE and the removal of heavy REE, as can be seen from the steeper curves in Figure 3c, and also the higher initial $^{87}Sr/^{86}Sr$ values in the rocks of the basement, the Kitoi Series, and the Onot greenstone belt (Table 9).

The petrogeochemical specific features of the rocks of the postultrametamorphic phase were controlled by the following factors: (1) the compositions of the replaced rock; (2) the chemical trends of the transformation processes accompanied by the redistribution of elements under the action of solutions enriched in H_2O, F, Cl, CO_2, and S; (3) the general physico-chemical conditions [*Levitskii,* 2000; *Petrova and Levitskii,* 1984]. These factors were responsible for the fact that the rocks of this group are extremely diverse in mineral and chemical compositions. They have highly variable and rather high $(^{87}Sr/^{86}Sr)_0$ values, indicative of a complex interaction between the crust and mantle materials and, probably, of isotope fractionation in zoned bodies. The early associations are represented by high-temperature and high-pressure assemblages, the late, by medium- and low-temperature and high-pressure rocks. Compared with the initial material, the rocks of the back zones are enriched in SiO_2 and (or) in Al_2O_3, and those from the marginal zones, in CaO and MgO. As the temperature of metasomatism declined (some temperature subclasses were replaced by others), the rocks were depleted in bases, alkalis, F, and Cl and enriched in SiO_2, H_2O, CO_2, and S. Generally the processes of postultrametamorphic transformations were accompanied by the redistribution of most petrogenic and trace elements.

The AFM diagram displayed in Figure 4 shows the mean compositions of the rocks from the Onot and Targazoi greenstone belts. They have similar characteristics: a calc-alkalic and a tholeiitic trend of the differentiation of the basic volcanogenic rocks and a growth of alkali metals and silica in the rocks of the ultrametamorphic phase.

In terms of their alkalis contents, the domination of K over Na, and Fe over Mg, the REE contents and distribution pattern (Figure 3), and their $(^{87}Sr/^{86}Sr)_0$ values, the granitoids of the Shumikha Complex resemble rapakivi granites, especially the well-known rapakivi-like granites of the Primorskii Complex [*Levitskii et al.,* 1997a]. This affinity is supported by the high Fe contents of their biotites (64–86%) and amphiboles (77–88%), and also by the elevated content of K_2O (0.9–2.3%) in amphiboles and of Al_2O_3 (13–16%) in biotites.

The rocks of the ultrametamorphic and post-ultrametamorphic phases and the granitoids of the Shumikha Complex showed similar petrogeochemical features: elevated K, Ba, Sr, Zr, Nb, TR, Pb, and Sn contents, enrichment in light and depletion in heavy REE (Figure 3), and the $(^{87}Sr/^{86}Sr)_0$ values higher than in the source rocks. These features suggest their genetic association with the same mantle sources. This seems to have controlled a change from the substantially Na-mafic specifics of the previously formed oceanic and continental crust to a K-alumosilicate specifics which was responsible for the formation of the garnet–metamorphic layer.

The compositions of metasomatic rocks from the zones of deep faults in the rocks of the Onot greenstone belt, similar to those of the postultrametamorphic phase, were controlled by the physicochemical conditions of their formation. A specific feature of the formation of the metasomatic rocks in the deep fault zones was the redistribution of petrogenic and trace elements, and also their removal and accumulation under more favorable conditions. For instance, the formation of the alumosilicate metasomatites after gneisses (granites, migmatites) was accompanied by the removal of SiO_2, alkalis, iron (after amphibolites), and almost all trace elements, which accumulated in the zones of the formation of apocarbonate metasomatites, and also of metalliferous apoamphibolite, apomigmatite, and apogranitoid rocks with Co, Ni, Cr, Au, Pd, Sn, and Be. Generally, the metasomatic rocks of the deep fault zones are much higher, compared with the source rocks, in F, S, B, and Zr and in some cases in Sn, Ta, Be, and Hf, this fact suggesting their addition in the course of the petrogenesis. These rocks usually have an abnormally high $(^{87}Sr/^{86}Sr)_0$ value. Of fundamental importance is also the fact that the formation of the Onot greenstone belt and the development of the metasomatic rocks in it took place at different times and were not related genetically.

The structural and petrogenic features of rocks and the formation mechanisms of greenstone belts and rifts are known to be similar in many respects [*Grachev,* 1977; *Grachev and Fedorovskii,* 1970; and many other authors]. A hot discussion in the 1980s [*Grachev and Fedorovskii,* 1970; *Keller et al.,* 1983; *Upton and Blundell,* 1978; to name but a few] on the topic of whether greenstone belts evolved from rift zones or island arcs resulted in the fact that at the present time most of investigators admit, though with significant reservations, the rift origin of greenstone belts, in general, [*Bozhko,* 1986; *Khain and Bozhko,* 1988; *Milanovskii,* 1983; and others], and of the Onot greenstone belt, in particular [*Mekhanoshin,* 1999; and others].

In the last decade some geoscientists succeeded in developing alternative models for the origin and evolution of greenstone belts from the standpoints of plate and plume tectonics [*Borukaev,* 1996; *Condie,* 1992; *Dobretsov and Kirdyashkin,* 1994, 1995; *Kroner,* 1991; *Sleep,* 1992; and others]. These models provide a more complete explanation of the main features of the structure, evolution, and composition of all observed rock complexes that superseded one another over a period of almost 3 Ga. During the early 3.1–3.7 Ga period of time a differentiated oceanic (metatholeiite) crust, represented by the rocks of the Sharyzhalgai Series, and a continental sialic tonalite–trondjemite crust existed in the region. It was only the continental crust that experienced active extension and sagging [after *Milanovskii,* 1983] and later (2.6–2.7 Ga) the formation of a suprastructure—the Onot, Targazoi, Monkres, and Urik–Iya greenstone belts with the greatly varying proportions and compositions of sedimentary and volcanic rocks, bordering the margins of the Sayan Salient of the Siberian Craton. That period of time was dominated by plastic deformations during the formation of troughs at the early stages of the history. The accumulation of the rocks of that complex occurred at the expense of both the intrusion of bimodal series and the destruction and disintegration of the sialic (tonalite–trondjemite) and mafic [essentially tholeiite; *Petrova and Levitskii,* 1984] materials. The rocks of the Kitoi Series, represented mainly by medium- and high-Al gneisses, marbles, and insignificant metabasalts, accumulated at the expense of the destruction of the Sharyzhalgai rocks. Later, the rocks of both series underwent granulite-facies metamorphism. The marginal parts of the structures tracing the junction zone between the greenstone belt and the basement rocks experienced, within the belt, intensive isochemical metamorphism (possibly to a granulite facies), and allochemical ultrametamorphism. Those were syncollision processes which operated during the interaction and collision of different, now consolidated blocks under the combination of extension and compression in different parts of the blocks and terminated the cratonization of the crust. These zones experienced intensive development of postultrametamorphic high-pressure metasomatites and postkinematic rapakivi-like A-type granites in the time interval of 2.0–1.8 Ga. Their development reflected the high alkali–potassic specifics of ancient rift-like systems. The latest rocks (633 Ma) are the low-T metasomatic rocks in the zone of the Main Sayan Fault. Its trend coincides with the trend of the junction zone between the granulite–gneiss and granite–greenstone regions, and also with the trend of the Cenozoic and Neogene basalts in the Tunkinskii Rift [*Grachev,* 1977]. This suggests paragenetic relations of petrogenesis in this region with mantle sources, possibly with long-lived low-density mantle diapirs [after *Bozhko,* 1986] in ancient and young rift-related structures.

Conclusion

1. The Early Archean period of the region's history was marked by the coexistence of the continental sialic crust represented by the tonalite–trondjemite rock associations in the basement of the Onot greenstone belt and of the oceanic (mafic) crust consisting of the rocks of the Sharyzhalgai Complex, which were later metamorphosed in the conditions of the granulite facies. The continental crust in the south of the Siberian Craton basement is composed of the rocks of a tonalite–trondjemite complex, the high-grade metamorphic rocks of the Kitoi Series, the rocks of the Onot greenstone belt, the rocks of the ultrametamorphic stage, the gabbroids of the Arban Complex, the metamorphosed ultramafics of the Ilchir Complex, the rocks of the post-ultrametamorphic stage, and the metasomatic rocks of the deep fault zones.

2. The Onot greenstone belt originated on the early sialic tonalite–trondjemite crust. Its base consists of calc-alkalic rocks ranging from rhyolites to basalts. Its middle interval includes tholeiitic metabasalts, clastic sediments, and carbonate facies which accumulated in shallow-sea areas and lagoons. The top of the sequence is highly dominated by clastic rocks. The rocks of the Kitoi Series accumulated simultaneously with the emplacement of the rocks of the Onot greenstone belt as a result of the disintegration and redeposition of the rocks of the Sharyzhalgai Complex.

3. The processes of the ultrametamorphic and post-ultrametamorphic transformations were of a superimposed allochemical character and made a significant contribution to the formation of the granite–metamorphic layer of the continental crust. The rocks of the post-ultrametamorphic stage accumulated under high-pressure conditions in the zones where geological structures of different age, metamorphism, and genesis contacted one another. The metasomatic rocks of deep fault zones and the ores they contain were not associated genetically with the formation of the Onot greenstone belt.

4. The rocks of the Shumikha Complex, classified here as rapakivi-like granites, are restricted to a contact between the Baikal granulite–gneiss region and the East Sayan granite–greenstone region. They are similar to the granites of the Primorskii Complex developed in the West Baikal region.

5. The contact zones between the East Sayan granite–greenstone and the Baikal granulite–gneiss regions show the linear bedding of the Onot rocks and the subconcordant alignment along these trends of the maximum development of the ultrametamorphic and postultrametamorphic rocks, Shumikha granitoids, and deep fault-zone metasomatites. This suggests the deep origin of these rocks and their genetic association with mantle sources.

Acknowledgments. This work was supported by the Russian Foundation for Basic Research, grants 00-05-64216, 99-05-64892, and 00-15-985760.

References

Abramovich, G. Ya., and P. M. Khrenov, Evolution of Precambrian Magmatism and Metallogeny in Southeastern Siberia in *Problems of Precambrian Lithosphere Evolution*, pp. 289–299, Nauka, Leningrad, 1986 (in Russian).

Aftalion, M., E. V. Bibikova, D. R. Bowes, et al., Timing of Early Proterozoic Collision and Extension Events in the Sharyzhalgai Granite–Gneiss–Charnockite–Granulite Complex, Lake Baikal, USSR: U–Pb, Rb–Sr and Sm–Nd Isotopic Study, *J. Geol., 99,* 851–862, 1991.

Bibikova, E. V., V. Ya. Khil'tova, T. V. Gracheva, et al., The Age of the Sayan Greenstone Belts, *Dokl. Akad, Nauk SSSR, 267,* (5), 1171–1174, 1982.

Bibikova, E. V., T. I. Kirnozova, V. A. Makarov, et al., Age Benchmarks in the Evolution of the Sharyzhalgai Complex in the Baikal Region (U-Pb System of Zircons), in *Geology and Geochronology of the Precambrian in the Siberian Craton and Its Surroundings*), pp. 162–170, Nauka, Leningrad, 1990 (in Russian).

Bozhko, N. A., Proterozoic Rifting, in *Problems of Precambrian Lithosphere Evolution,* pp. 95–103, Nauka, Leningrad, 1986 (in Russian).

Borukaev, Ch. B., *Archean Plate Tectonics,* NITs OIGGM SO RAN, Novosibirsk, 1996 (in Russian).

Collerson, K. D., and D. Bridgewater, Metamorphic Evolution of Early Archean Tonalite and Trondjemite Gneisses in Saglek, Labrador, in *Trondjemites, Dacites, and Related Rocks*, pp. 157–203, Mir, Moscow, 1983 (Russian translation).

Condie, L., *Archean Greenstone Belts*, Mir, Moscow, 1983 (Russian translation).

Condie, K. C., Early Archean Greenstones and the Delayed Appearance of Cratons, in *29th Internat. Geol. Congr., Abstr.,* vol. 1, p. 3, 1992.

Condie, K. C., and D. R. Hanter, Trace element geochemistry of Archean granitic rocks from the Barberton region, South Africa, *Earth Planet. Sci. Lett., 29,* 389–400, 1976.

Dobretsov, N. L., and A. G. Kirdyashkin, *Deep Crustal Geodynamics*, NITs OIGGM SO RAN, Novosibirsk, 1994 (in Russian).

Dobretsov, N. L., and A. G. Kirdyashkin, Heat Transfer and Rheology of the Lower Mantle in the Early Periods of the Earth's Evolution, *Dokl. Akad. Nauk, 345,* (1), 103–105, 1995.

Emission Spectral Analysis in Geochemistry, Nauka, Novosibirsk, 1976 (in Russian).

Finkelshtein, A. L., and V. P. Afonin, Analytical Approximation for Calculating Secondary Fluorescence in X-Ray Analysis of Powdered Materials, *X-Ray Spectrom., 25,* 156–199, 1996.

Glebovitskii, V. A., and S. A. Bushmin, *Postmigmatite Metasomatism*, Nauka, Leningrad, 1983.

Gornova, M. A., and Z. I. Petrova, Mantle Peridotites of a Granulite–Gneiss Complex as Fragments of Archean(?) Ophiolites in the Baikal Region, *Ofioliti, 24,* (2), 223–238, 1999 (in Russian).

Grabkin, O. V., and S. A. Melnikov, *Structure of the Basement of the Siberian Craton in the Zone of a Marginal Suture*, Nauka, Novosibirsk, 1980 (in Russian).

Grachev, A. F., *Rift Zones of the Earth*, Nedra, Leningrad, 1977 (in Russian).

Grachev, A. F., and V. S. Fedorovskii, On the Common Origin of Rifts, Aulacogens, and Geosynclinal Troughs, *Sov. Geologiya,* (12), 121–122, 1970.

Grachev, A. F., and V. S. Fedorovskii, Precambrian Greenstone Belts: Rifts or Island Arcs?, *Geotektonika,* (12), 3–22, 1980.

Hanter, D. R., The Role of Tonalites and Trondjemites in the Formation of the Earth's Crust in Swaziland and Transvaal, South Africa, in *Trondjemites, Dacites, and Related Rocks*, pp. 223–238, Mir, Moscow, 1983 (Russian translation).

Hanter, D. R., et al., The Geochemical Nature of the Archean Ancient Gneiss Complex and a Granodiorite Suite, Swaziland: A Preliminary Study, *Precambr. Res., 7,* 105–127, 1978.

Keller, D. R., E. G. Lidiak, W. J. Hinze, and L. M. Braile, The Role of Rifting in the Tectonic Development of the Midcontinent, USA, *Tectonophysics, 94,* 391–412, 1983.

Khain, V. E., and N. A. Bozhko, *Historical Tectonics of the Precambrian*, Nedra, Moscow, 1988 (in Russian).

Kirnozova, T. I., V. I. Levitskii, A. I. Melnikov, et al., The U–Pb Age of the Sayan Granites in the Biryusa Block, in *Isotope Dating of Geologic Processes: New Methods and Solutions*, pp. 178–180, Moscow: Proc. 1st Ross. Conf. on Isotope Geochronology, 2000 (in Russian).

Kroner, A., Tectonic Evolution in the Archean and Proterozoic, *Tectonophysics, 187,* (4), 393–410, 1991.

Levitskii, V. I., Petrology, Mineralogy, and Genesis of the Onot Talc Deposit, *Zapiski Vseros. Min. Ob-va, CXXIII,* (6), 20–32, 1994.

Levitskii, V. I., Geochemistry of Metasomatism and Its Role in the Formation of the Continental Crust, *Doctoral (Geol.) Dissertation*, p. 566, Institute of Geochemistry, Sib. Div. Acad. Nauk, Irkutsk, 2000.

Levitskii, V. I., G. P. Sandimirova, and Yu. A. Pakholchenko, Succession of Endogenic Processes in the Granulite–Gneiss and Granite–Greenstone Complexes of the East Sayan Region, in *Russian Foundation for Basic Research (Earth's Crust and Mantle), Petrology, Geochemistry, and Mineralogy*, pp. 76–77, IZK SO RAN, Irkutsk, 1995 (in Russian).

Levitskii, V. I., L. A. Pavlova, and G. P. Sandimirova, Rapakivi-like Granitoids of the Southeast Sayan Region, in *Granitoid Volcanoplutonic Associations* (Abstracts, All-Russia Conference, Institute of Geology, Komi Scientific Center, Uralian Div. Russian Academy of Sciences, Syktyvkar), pp. 124-125, 1997a (in Russian).

Levitskii, V. I., L. A. Pavlova, and G. P. Sandimirova, Granitoids of the Shumikha and Primorskii Complexes: Correlation, Mineralogy, and Geochemistry, in *Abstr. 6th East Siberian Regional Conf. on Petrography*, IGU, Irkutsk, 1997b.

Lobachevskii, I. V., and A. I. Melnikov, The Structure of the Basement in the Angara–Oka Sayan Region from Geological and Geophysical Data, *Sov. Geologiya,* (5), 36–45, 1985.

McIntyre, G. A., G. Brooks, W. Compston, and A. Turek, The Statistical Assessment of Rb–Sr Isochrons, *J. Geophys. Res., 71,* (22), 5459–5468, 1966.

Mac-Gregor, W. P., Archean Gray Gneisses and the Origin of Continental Crust: Evidence from Gothob, Western Greenland, in *Trondjemites, Dacites, and Related Rocks*, pp. 131-156, Mir, Moscow 1983 (Russian translation).

Mekhanoshin, A. S., The Basic–Ultrabasic Magmatism of the Onot Greenstone Belt (Eastern Sayan), *Geologiya i Geofizika, 40,* (12), 1772–1784, 1999.

Mekhanoshin, A. S., G. P. Sandimirova, G. S. Plyusnin, et al., New Data on the Rb–Sr Geochronology of the Sharyzhalgai Rocks (Southwest Baikal Region), in *Geology and Geochronology of the Precambrian in the Siberian Craton and Its Surroundings*, pp. 209–210, IZK SO RAN, Irkutsk, 1987 (in Russian).

Melnikov, A. I., Sharyzhalgai Structural Zone in the South of the Siberian Craton (Baikal Region), in *Granulite Complexes of Continental Crust*, pp. 71–92, Nauka, Moscow, 1991 (in Russian).

Milanovskii, E. E., *Rifting in the Earth's History*, 279 p., Nedra, Moscow, 1983 (in Russian).

Monin, A. S., The Early History of the Earth, 261 pp., Nedra, Moscow, 1987 (in Russia).

Nonmetallic Mineral Deposits of the USSR, Nedra, Moscow, 1984 (in Russian).

Nozhkin, A. D., V. I. Levitskii, A. S. Mekhanoshin, et al., Geochemistry of Early Archean Granitoids and Metavolcanic Sediments in the Onot Greenstone Belt (Southeast Sayan Region), *Geol. Geofiz., 36,* (3), 45–54, 1995.

Petrova, Z. I., Geochemistry of Granulite–Gneiss Complexes, *Doctoral (Geol.) Dissertation,* IGKh SO AN SSSR, Irkutsk, 1990.

Petrova, Z. I., and V. I. Levitskii, *Petrology and Geochemistry of Granulite Complexes in the Baikal Region,* Nauka, Novosibirsk, 1984 (in Russian).

Poletaev, I. A., Metasomatic Processes and Structural Control during the Formation of the Savina Co-bearing Massive Sulfide Deposit, *Doctoral (Geol.) Dissertation,* IPI, Irkutsk, 1973.

Precambrian and Paleozoic Evolution of the Earth's Crust in the Sayan–Baikal Fold Region, Nauka, Novosibirsk, 1988 (in Russian).

Sandimirova, G. P., G. S. Plyusnin, Z. I. Petrova, et al., The Rb–Zr Age of the Rocks of the Sharyzhalgai Series, in *Izotope Geology of the Precambrian*, pp. 160–161, IGN, Ufa, 1979 (in Russian).

Sandimirova, G. P., V. I. Levitskii, Yu. A. Pakholchenko, et al., Rb–Sr Geochronology of the Oldest Granitoids in the East Sayan Region, *Dokl. Akad. Nauk SSSR, 326,* (4), 696–700, 1992.

Sandimirova, G. P., V. I. Levitskii, Yu. A. Pakholchenko, et al., The Rb–Sr Age and Geochemistry of the Oldest Granitoids in the Onot–Savina Area of the Sayan Region, in *Isotope Dating of Endogenic Metalliferous Rocks*, pp. 92–102, Nauka, Moscow, 1993 (in Russian).

Shames, P. I., Eastern Sayan Tectonics, in *Geology of the USSR, Irkutsk Region*, Moscow: Gosgeoltekhizdat, vol. 27, pp. 136–186, 1962 (in Russian).

Sharkov, E. V., O. A. Bogatikov, V. I. Kovalenko, et al., Early Precambrian Lower-Crust Basic Granulites and Eclogites: Examples from the Kola Peninsula and Southern Sayan Region, *Geologiya i Geofizika, 37,* (1), 94–113, 1996.

Shafeev, A. A., Yu. A. Buinov, and A. A. Gorelov, Sizes and Forms of Metasomatism in Deep Fault Zones, in *Petrology and Mineralogy of Metamorphic Rocks in Eastern Siberia*, pp. 106–123, Nauka, Novosibirsk, 1981 (in Russian).

Shcherbakov, A. F., and I. A. Poletaev, Magnesite Ore from the Savina Deposit, *Litol. Polezn. Iskop.,* (6), 16–27, 1977.

Sleep, N. H., Archean Plate Tectonics: What Can Be Learned from Continental Geology?, *Canad. J. Earth Sci., 29,* (10), 2066–2971, 1992.

Smirnova, E. V., and V. V. Konusova, Spectral and Chemico-Spectral Determination of Rare Earth Elements in Rocks, in *Geochemistry of Rare Earth Elements in Endogenic Processes*, pp. 3–31, Nauka, Novosibirsk, 1982 (in Russian).

Tauson, L. V., V. N. Sobachenko, G. S. Plyusnin, et al., The Rb–Sr Age of Rapakivi-like Granitoids and Metasomatic Rocks in the Kvatugino–Ayan Zone, *Dokl. Akad. Nauk SSSR, 273,* (5), 1233–1236, 1983.

Trondjemites, Dacites and Related Rocks, Mir, Moscow, 1983 (in Russian).
York, K. D., Least-Squares Fitting of a Straight Line, *Canad. I. Phys.*, *44*, (5), 1079–1086, 1966.
Upton, B. G., and D. J. Blundell, The Gardar Igneous Province: Evidence for Proterozoic Continental Rifting, in *Petrology and Geochemistry of Continental Rifts,* pp. 163–172, Dordrecht, 1978.

(Received August 10, 2001)